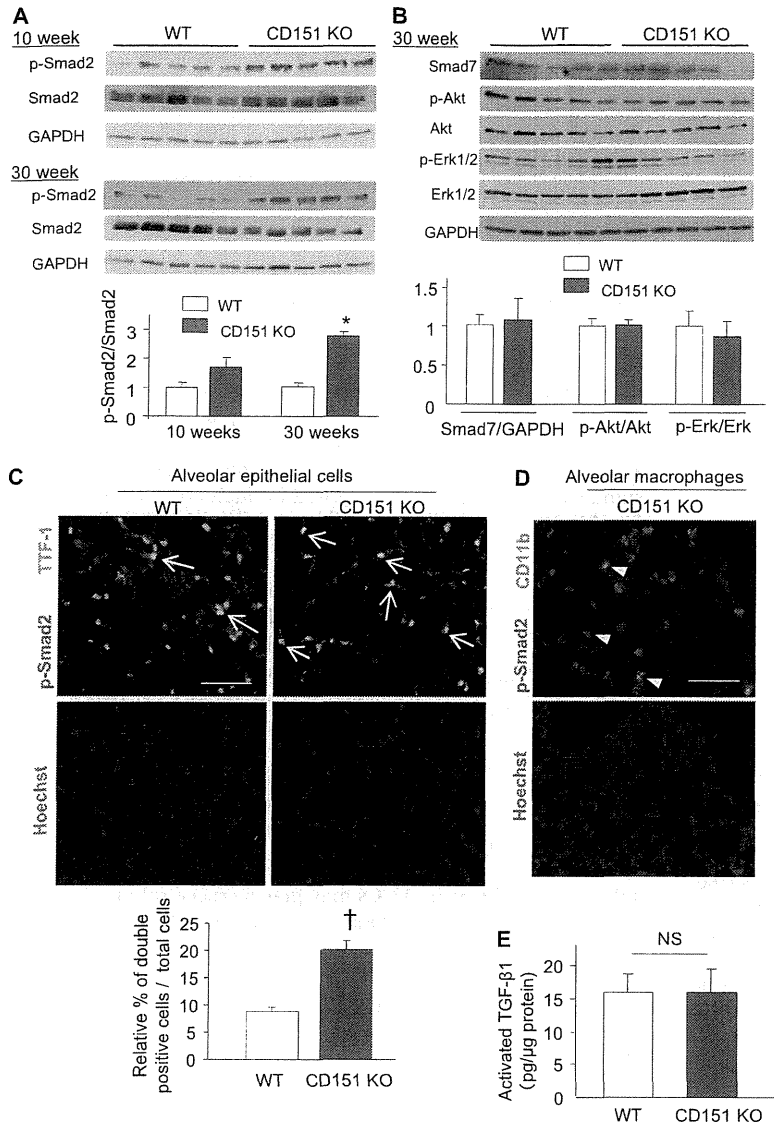

Figure 3. Enhanced p-Smad2 signaling in the alveolar epithelial cells (AECs) of CD151 knockout (KO) mice. (*A*) Western blot analysis and densitometric quantification of p-Smad2 in total protein homogenates from wild-type (WT) and CD151 KO lungs. Values of p-Smad2 were normalized against total Smad2. $^{*}P < 0.001$. (*B*) Western blot analysis and densitometric quantification of Smad7 and p-Akt in total protein homogenates from WT and CD151 KO lungs. Values of Smad7, p-Akt, and p-Erk1/2 were normalized against GAPDH, Akt, and Erk, respectively. (*C*, *D*) Immunofluorescence of mouse lungs stained for p-Smad2 and TTF-1 or CD11b. The numbers of p-Smad2 and TTF-1 double-positive AECs (*arrows*) were significantly larger in CD151 KO lungs (*C*, n = 4 per group, $^{\dagger}P < 0.05$). p-Smad2–positive signals were scarcely seen in CD11b-positive alveolar macrophages (*D*, *arrowheads*). Bar = 100 μm. (*E*) Activated TGF-β_1 in whole lung was measured by ELISA and normalized against total protein. Levels of activated TGF-β_1 were comparable between WT and CD151 KO lungs (n = 3 per group).

Matrigel/BM. CD151-deleted AECs adhered onto ECM similarly to control cells (Figure 4B). However, they were easily detached by chemical and mechanical forces when grown on Matrigel, but not fibronectin (Figures 4C and 4D), suggesting that the adhesion strengthening of CD151-deleted AECs on Matrigel was impaired. On the other hand, deletion of CD151 in AECs did not affect random migration, wound closing assays, proliferation, or exogenous TGF-β_1–induced signaling (Figure E4). Collectively, the data suggest that the presence of CD151 in AECs is required for firm adhesion to BM.

CD151 Is Necessary for AECs to Maintain Epithelial Characteristics on BM

Adhesion to BM was indispensable in order for epithelial cells to maintain their epithelial integrity (22, 23). Indeed, in the presence of serum, AECs maintained epithelial characteristics on Matrigel; in contrast, on collagen-1–, fibronectin-, or non-ECM–coated dishes, they exhibited elevation of p-Smad2 and mesenchymal-like changes, namely, increased α-SMA and decreased E-cadherin (Figure 5A). Again, these findings indicate that adhesion to Matrigel, but not collagen/fibronectin, protects AECs against mesenchymal changes and up-regulation of TGF-β signaling. However, these protective roles of Matrigel were overcome in the presence of a large amount of TGF-β_1 (Figure 5A). Of note, CD151-deleted AECs lost epithelial integrity on Matrigel; they exhibited an enlarged morphology and increased α-SMA expression concomitant with upregulation of p-Smad2 levels, similar to cells treated with TGF-β_1 (Figures 5B and 5C). These effects of CD151 deletion were not obvious on fibronectin-coated dishes, indicating that they might result from attenuated interaction with Matrigel. Consistent with this, α-SMA and pro-SPC double-positive cells were observed in CD151 KO lungs, but not in WT lungs, suggesting that these cells were in a state of epithelial-to-mesenchymal transition (EMT; Figure 5D). Furthermore, AECs isolated from CD151 KO mice exhibited relatively higher α-SMA expression (Figure 5E). Taken together, our data suggest that CD151 is required in order for AECs to preserve their integrity by maintaining firm adhesion to BM.

Deletion of CD151 Does Not Affect Lung Fibroblast Function

Because resident fibroblasts are believed to be the main source of collagen-secreting myofibroblasts in pulmonary fibrosis (24), we investigated the functional role of CD151 in primary lung

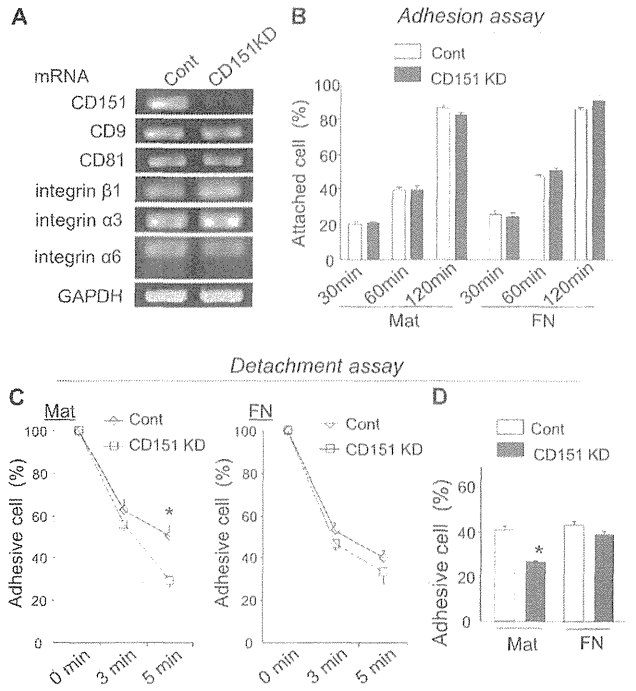

Figure 4. Deletion of CD151 results in attenuated adhesion strength of alveolar epithelial cells (AECs) on Matrigel. (*A*) The expression of CD151 was significantly down-regulated in CD151 knockdown (KD) AECs compared with cells treated with control siRNAs (cont). No significant change was observed in the expression of other tetraspanins (CD9, CD81) and associated integrins (β1, α3, and α6). (*B*) AECs were seeded on Matrigel (Mat)- or fibronectin (FN)-coated 96-well plates for 30, 60, and 120 minutes. After medium was gently changed, the attached cells were counted. The number of attached cells is shown in relation to total seeded cells. CD151 KD cells adhered to Mat and FN similarly to cont. (*C, D*) Adhesion strength of AECs on Mat is attenuated by CD151 knockdown. Trypsin/EDTA-induced (*C*) or mechanical vibration–induced (*D*) detachment was enhanced in CD151 KD cells cultured on Mat but not on FN. $^*P < 0.05$. Data are representative of three independent experiments, which yielded similar results.

fibroblasts. Although fibroblasts from CD151 KO mice exhibited increased migration on Matrigel, the effect did not reach statistical significance. Otherwise, we could not see any differences between primary fibroblasts isolated from WT and CD151 KO lungs regarding chemotaxis, proliferation, differentiation into myofibroblasts, or collagen production (Figure E5).

BLM Injury Exacerbates AEC Disintegrity in CD151 KO Mice, Followed by Severe Pulmonary Fibrosis with Increased Mortality

We next examined the significance of CD151 under intratracheal BLM exposure, which initially causes direct injury to AECs and ultimately leads to pulmonary fibrosis (25). Low-dose intratracheal BLM induced a moderate decrease in CD151 expression in WT lungs and a gradual increase in collagen-1 expression (Figure E6). In CD151 KO lungs, BLM treatment caused enlargement of AECs, and their α-SMA expression was dramatically increased (Figure 6A), suggesting that disintegrity of AECs was accelerated by BLM injury. On the other hand, the number of inflammatory cells in bronchoalveolar lavage fluid of CD151 KO lungs was only mildly increased (Figure 6B). Accelerated epithelial disintegrity was followed by severe fibrosis in CD151 KO lungs, as was evident from histopathology, CT scan, increased hydroxyproline content, and decreased lung compliance (Figures 6C–6F). Furthermore, these changes resulted in increased and prolonged body weight loss (Figure 6G) and severe mortality (Figure 6H). Nevertheless, BLM-induced fibrosis in CD9 KO mice was not increased compared with that in WT mice, although the number of lung inflammatory cells increased (Figure E7).

In summary, disintegrity of AECs in CD151 KO lungs was further exacerbated by BLM exposure, ultimately resulting in severe fibrosis.

CD151 Expression Is Significantly Decreased in Human AECs from Patients with IPF

Finally, to investigate the possible involvement of CD151 in human pulmonary fibrosis, we analyzed lung sections from patients with IPF/usual interstitial pneumonia. P-Smad2 staining from lung sections from patients with IPF revealed increased positive signals relative to healthy lungs (Figures 7A and 7D). These signals in IPF lungs were enriched in nuclei of AECs (Figures 7A–7F, Figure E8), implying that TGF-β_1 signaling in AECs might play an important role in the development of human pulmonary fibrosis.

In our quantitative polymerase chain reaction analysis using human lung homogenates, we detected no significant difference in CD151 expression levels between healthy and IPF lungs (Figure E9). In immunofluorescence, however, most AECs in healthy lung tissues expressed CD151 (Figure 7G), whereas CD151-negative AECs could be focally observed in IPF lungs (Figures 7H–7L). Histological quantitation revealed fewer CD151-positive AECs in lung samples from patients with IPF compared with healthy lungs (Figure 7M), although CD151 expression levels fluctuated. In contrast, CD151 expression in alveolar macrophages was comparable between the two groups. Taken together, these observations indicate that CD151 in AECs may play a crucial role in the pathogenesis of pulmonary fibrosis in humans as well as mice.

DISCUSSION

Here, we provide new evidence that CD151 KO mice spontaneously develop age-related pulmonary fibrosis, which is exacerbated by BLM exposure. To date, it has been reported that CD151 KO mice have renal dysfunction (in the FVB strain) (26–28), impaired pathologic angiogenesis (15), delayed wound closure (29), and deficiencies in platelet aggregation (30). However, the involvement of CD151 in lung diseases remains unclear; this is the first report implicating CD151 in protection against pulmonary fibrosis. We also observed focal fibrotic changes in the kidneys and liver of CD151 KO mice, further supporting the critical role played by CD151 in fibrosis.

Accumulating evidence suggests that in addition to intrinsic factors in host lungs (i.e., genetic predisposition), extrinsic factors that accelerate injury of AECs also play an etiologic role in IPF. These factors include environmental exposure, transbronchial infection, and aging (2, 3, 31, 32). Our results fit this idea well because the fibrotic phenotype and epithelial disintegrity of CD151 KO mice became more evident with increased age and was exacerbated by low-dose BLM exposure. In contrast to CD151 KO mice, however, patients with IPF do not commonly present with kidney and liver symptoms. In some IPF lungs, we found that CD151 expression is focally decreased in AECs but not in alveolar macrophages, suggesting that CD151 down-regulation in AECs is the result of an extrinsic factor, rather than a genetic factor. Consistent with this idea, intratracheal BLM decreased CD151 expression in the lung. Recently, hypoxic stress was shown to down-regulate CD151 expression in colon cancer cells through the up-regulation of hypoxia-inducible factor-1 (HIF-1) (33). Likewise, in AECs, we showed that hypoxic

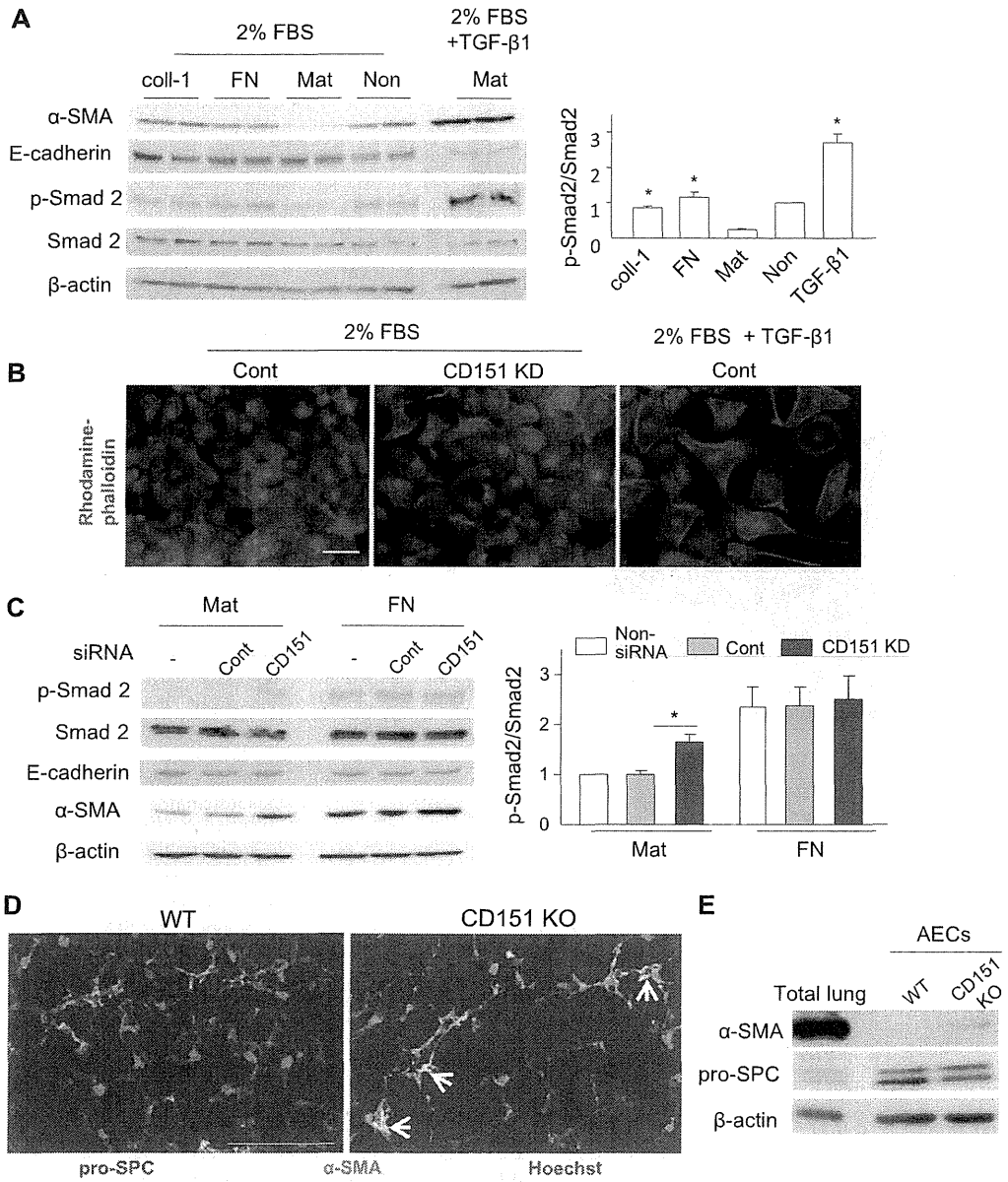

Figure 5. Deletion of CD151 causes disintegrity of alveolar epithelial cells (AECs) on basement membrane, with increased α-SMA expression and transforming growth factor (TGF)-β signaling. (*A*) AECs isolated from H-2K^b-tsA58 transgenic mice were cultured on collagen-1 (coll-1)–coated, fibronectin (FN)-coated, Matrigel (Mat)-coated, and noncoated (Non) dishes. After incubation for 72 hours in Dulbecco's modified Eagle medium with 2% fetal bovine serum, only AECs cultured on Mat maintained an epithelial character and lower p-Smad2 signaling. As a control, AECs were stimulated with 10 ng/ml of TGF-β_1 for 48 hours on Mat. In the densitometric quantitation, values of p-Smad2 were normalized against Smad2 and divided by values obtained on noncoated dishes (n = 4 per group). *$P <$ 0.01 (vs. Mat). (*B*) The morphology of AECs cultured on Mat was analyzed by rhodamine-phalloidin staining. Compared with AECs treated by control siRNAs (cont), CD151 knockdown (KD) cells exhibited enlarged morphologies similar to those observed in cells treated by TGF-β_1. After 48 hours of treatment with TGF-β_1 (10 ng/ml), AECs lost their epithelial integrity and exhibited mesenchymal-like changes; they became enlarged and spindle-shaped, and actin filaments formed stress fibers. Bar = 20 μm. (*C*) Deletion of CD151 caused up-regulation of p-Smad2 levels, with increased α-SMA expression, in AECs on Mat, whereas these effects of CD151 deletion were not obvious on FN. *$P < 0.05$. Data are representative of three independent experiments, which yielded similar results. (*D*) In immunofluorescence analyses of frozen lung sections, epithelial cells expressing both pro-SPC and α-SMA were observed in CD151 knockout (KO) lungs, suggesting that they were in a state of epithelial-to-mesenchymal transition. However, no epithelial cells in the lung tissues of wild-type (WT) mice exhibited α-SMA expression. Bar = 100 μm. (*E*) AECs isolated from CD151 KO lungs exhibited higher expression of α-SMA than ones from WT lungs. Representatives of at least three similar results were shown.

stress down-regulates CD151 expression (Figure E10). It has become clear that HIF-1 is significantly up-regulated in AECs of IPF and BLM-induced fibrotic mouse lungs (34). In this context, hypoxic stress and subsequent up-regulation of HIF-1 are one possible cause of focal decrease of CD151 in IPF lungs. However, the expression levels of CD151 appeared to differ among lungs from different patients with IPF. Fujishima and colleagues previously reported that CD151 expression in epithelial cells and macrophages is relevant to the activation of matrilysin-1 in IPF lungs (35). It thus appears that expression of CD151 in cases of pulmonary fibrosis depends on the site, clinical phase, and possible complications involving infection. Further investigation will be required to address the clinical significance of CD151 expression in IPF lungs.

Despite the increased number of lung inflammatory cells, CD9 KO mice did not exhibit severe fibrotic changes compared with WT mice, even after BLM exposure. These findings are in line with the idea that increased inflammation does not necessarily lead to augmented fibrosis. Double deletion of CD9 and a homologous tetraspanin, CD81, spontaneously leads to pulmonary emphysema in mice (10). Determination of the shared and distinctive pathways/molecules associated with CD151 and CD9 might help us to understand the pathogenesis of pulmonary fibrosis and emphysema.

We found that deletion of CD151 resulted in disintegrity of AECs, activated p-Smad2, and EMT-like changes, which might causally contribute to the development of pulmonary fibrosis. First, activation of TGF-β signaling in AECs may be a primary source of the development of pulmonary fibrosis, because mice with epithelial cell–specific loss of TGF-β receptor are protected from BLM-induced pulmonary fibrosis (36, 37). Consistent with

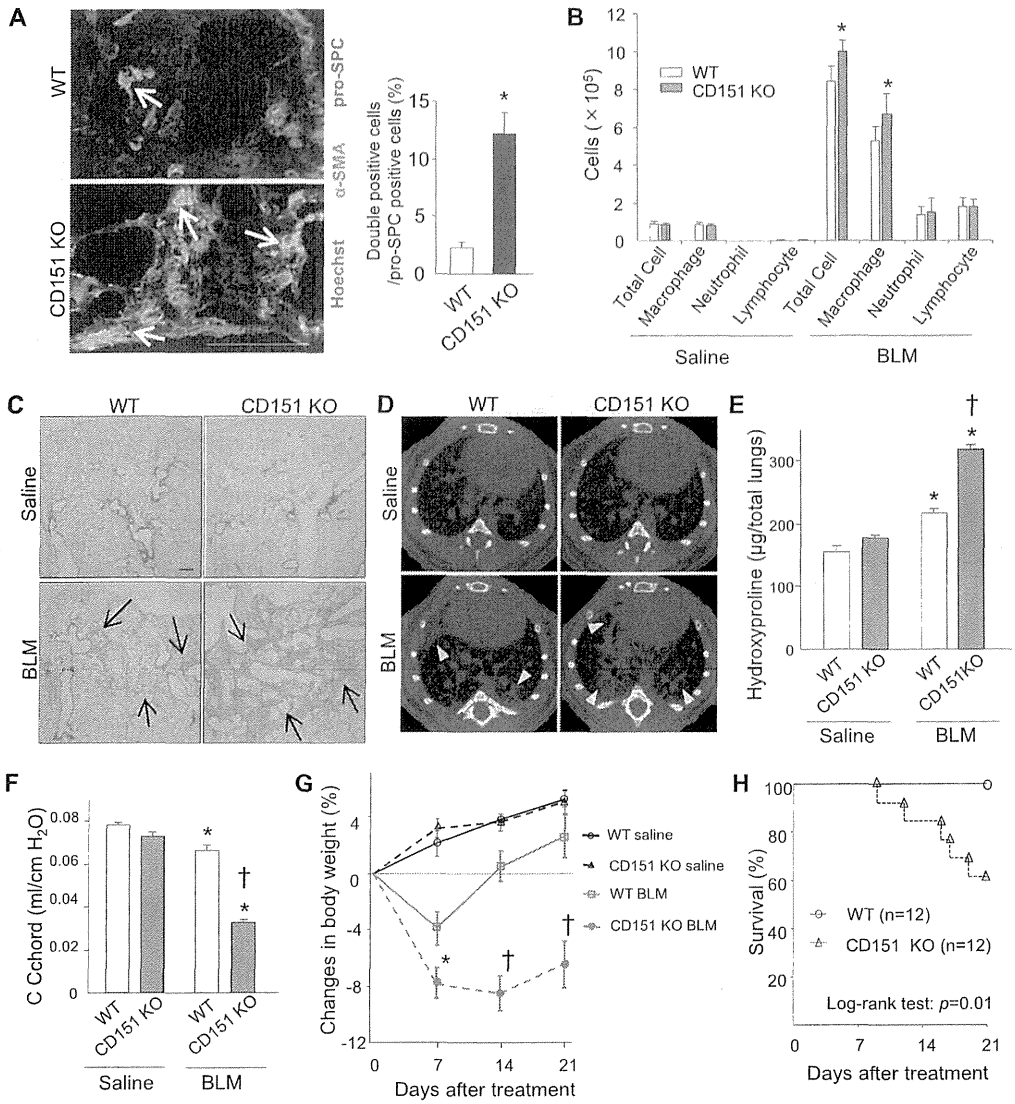

Figure 6. Low-dose bleomycin (BLM) injury accelerates epithelial disintegrity, followed by exacerbated pulmonary fibrosis in CD151 knockout (KO) mice. (*A*) Fourteen days after BLM injury (1.2 U/kg), alveolar epithelial cells (AECs) were deformed, and the proportion of AECs expressing both α-SMA and pro-SPC was significantly increased in CD151 KO lungs compared with wild-type (WT) (n = 4 per group, $*P < 0.01$). Bar = 100 μm. (*B*) Cell numbers in bronchoalveolar lavage fluids peaked 7 days after saline/BLM treatment. CD151 KO mice exhibited mildly increased lung inflammatory cells relative to WT mice after BLM injury (n = 4–6 per group). $*P < 0.05$ (vs. WT). (*C, D*) Twenty-one days after BLM injury, increased lung fibrosis was observed in both WT mice and CD151 KO mice compared with their saline controls, but this phenomenon was much more severe in CD151 KO mice, as indicated by histopathology (hematoxylin-eosin staining, *C, arrows*; bar = 100 μm) and computed tomography (*D, arrowheads*). (*E*) Hydroxyproline assays confirmed increased collagen content in total lungs after BLM treatment in CD151 KO mice relative to WT mice (n = 5–6 per group). $*P < 0.01$ (vs. saline), $^{\dagger}P < 0.001$ (vs. WT). (*F*) Twenty-one days after BLM injury, compliance (C chord) of CD151 KO lungs was significantly decreased to around half the WT level (n = 5–6 per group). $*P < 0.01$ (vs. saline), $^{\dagger}P < 0.001$ (vs. WT). (*G*) Changes in body weight after BLM injury. From 14 to 21 days after treatment, WT mice regained their weight, whereas the weight loss of CD151 KO mice continued. During the whole period of the experiment, saline control mice gradually gained weight (n = 4–6 per group). $*P < 0.05$ (vs. WT), $^{\dagger}P < 0.01$ (vs. WT). (*H*) After BLM injury, the mortality of CD151 KO mice was larger than that of WT mice (log-rank test: $P = 0.01$).

this, in our analyses of IPF lungs, activated p-Smad2 signals were predominantly observed in AECs. Second, myofibroblasts that arise from EMT could themselves contribute to the development of pulmonary fibrosis (38–40). Changes in CD151-deleted AECs were mild, but similar to those observed in cells treated with TGF-β_1, suggesting that CD151 deletion promotes EMT. In line with our study, CD151 deficiency in epithelial cells results in increased actin stress fibers at the basal cell surface and perturbs cell polarity (11, 41). In contrast, in hepatocellular carcinoma cells, the complex containing CD151 and α6β1 integrin promotes EMT (42). Further investigation will be needed to address the role of CD151 in EMT in normal and malignant cells.

We found that CD151 is essential for firm adhesion of AECs on BM. Among several ECM molecules contained in BM, laminin may be the most crucially involved in this adhesion, because CD151 determines the strength of cell–ECM interactions by forming complexes with laminin-binding integrins such as α3β1, α6β4, and α6β1 (43–45). We also found that this firm adhesion to BM protects AECs against EMT-like changes and up-regulation of p-Smad2. Likewise, during embryonic development, BM protects against EMT in primitive ectoderm (22), further supporting our results. However, we could not determine how loss of adhesion to BM leads to elevation of p-Smad2 in serum. Possible explanations include response to the low level of TGF-β_1 contained in serum or an increase in autocrine/paracrine TGF-β signaling from activated AECs exhibiting mesenchymal-like changes. In a previous study of breast cancer cells, CD151 was shown to regulate TGF-β_1–induced cell scattering and proliferation via activation of p38 (46). Additional studies will be required to elucidate how CD151 is involved in TGF-β_1 signaling in normal and malignant cells.

However, there may be alternative explanations for fibrotic changes, because CD151 is implicated in a variety of cell functions through its association with multiple proteins. First, CD151 modulates various integrin-dependent cell functions. Recently, mice were generated with lung epithelium–specific loss of α3 integrin expression (14). In contrast to CD151 KO mice, these mutant mice exhibited a blunted response to BLM injury, in

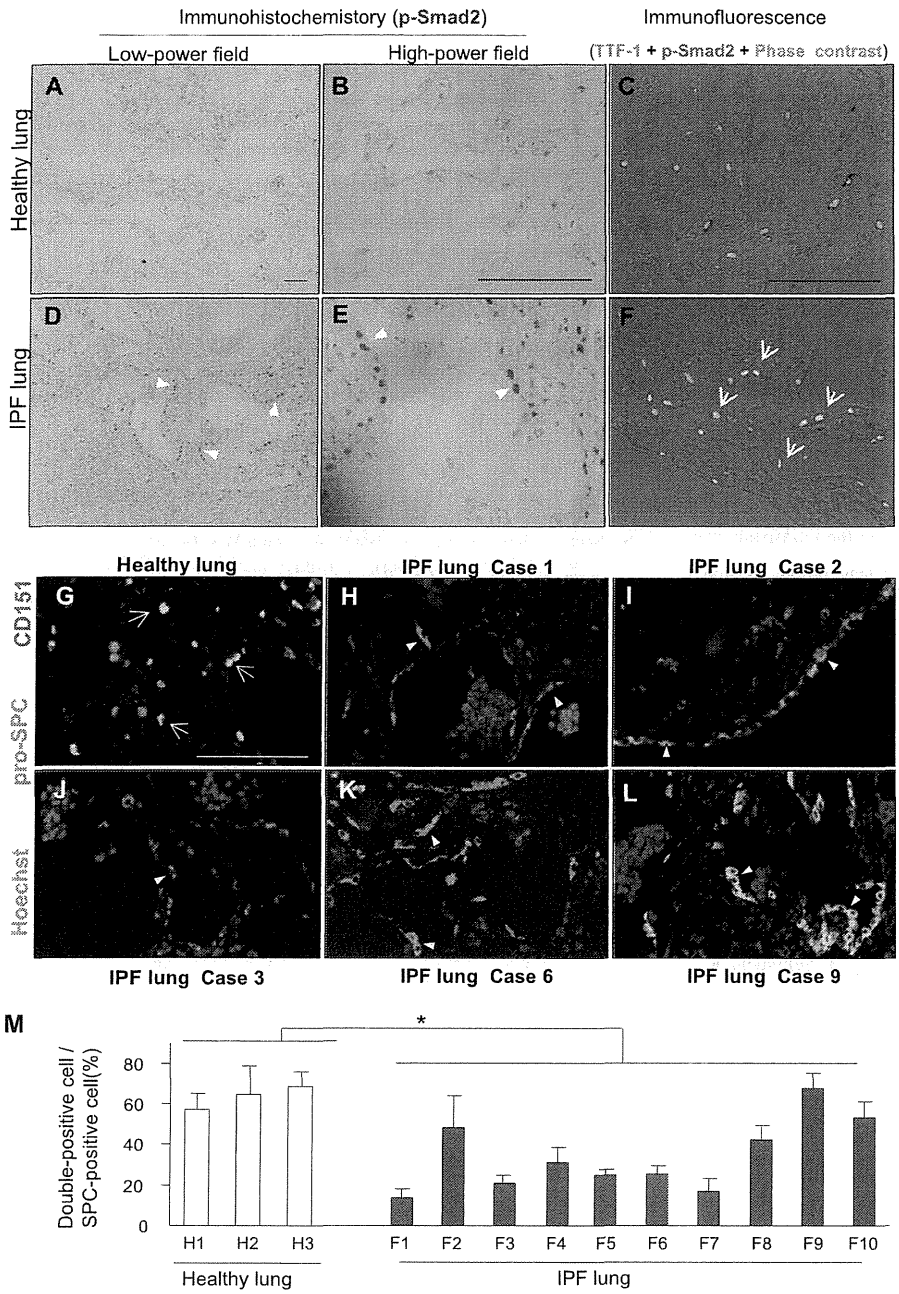

Figure 7. CD151 expression is significantly decreased in alveolar epithelial cells (AECs) from patients with idiopathic pulmonary fibrosis (IPF). (*A–F*) IPF lungs contained more p-Smad2 signals than healthy lungs (*A, D, arrowheads*). P-Smad2–positive signals of IPF lungs were preferentially observed in nuclei of AECs (*B, C, E,* and *F, arrowheads* and *arrows*). Representative IPF and healthy lung sections were shown. Bar = 100 μm. TTF-1 = specific marker for type II AECs. (*G–L*) Representative immunostaining of pro-SPC and CD151 in healthy (n = 3) and IPF (n = 10) lungs. Most AECs expressed CD151 in healthy lungs (*G, arrows*), whereas CD151-negative AECs were prominent in the lungs of IPF cases 1, 2, 3, and 6 (*H–K, arrowheads*). Notably, clear and diffuse expression of CD151 was observed in AECs in the lung of case 9 (*L, arrowheads*). Bar = 100 μm. (*M*) In histological quantification, at least three fields from each lung were randomly chosen, and an average of 50 pro-SPC–stained AECs per field were quantitated. The number of CD151-positive AECs was significantly decreased in the lungs of patients with IPF (F1–10) compared with healthy lungs (H1–3, $^*P < 0.05$).

which a CD151-independent function of α3β1 integrin could be involved. However, similar to our CD151 KO mice, the mutants exhibited increased collagen deposition in their lungs, suggesting that some functions mediated by CD151-α3β1 integrin complexes may be involved in the fibrotic phenotype of CD151 KO mice. Further study is warranted to determine how CD151 deletion affects the function of associated integrins. Second, other cells, such as resident fibroblasts, could contribute to the progression of fibrosis. However, as far as we could determine, CD151 is minimally involved in lung fibroblast functions related to fibrosis.

Consistent with a crucial role for CD151 in mouse pulmonary fibrosis, CD151 expression in patients with IPF is focally diminished in type II AECs. In addition, type II AECs in CD151 KO mice are hypertrophied and contain increased numbers of lamellar body–like structures, similar to what is observed in familial human IPF (47). These findings suggest that CD151 in AECs plays critical roles in the pathogenesis of pulmonary fibrosis, in humans as well as mice. Recently, a mutation in CD151 was reported in a few patients with Alport syndrome, who exhibit sensorineural deafness and pretibial epidermolysis bullosa (48). Our results suggest that these patients should also be assayed for fibrotic changes in the lungs.

In conclusion, we here provide evidence that CD151 is essential for AECs, and deletion of CD151 results in pulmonary fibrosis. To date, numerous transgenic mice overexpressing profibrogenic cytokines exhibit pulmonary fibrosis (25), whereas only a few molecules that play protective roles in pulmonary fibrosis have been identified in mouse models or in humans: SPC (47), caveolin-1 (49, 50), relaxin (51), and connexin (52). Most therapies for IPF targeted against profibrogenic cytokines have not been effective in clinical trials (53). Therefore, it may be reasonable to focus efforts on protective factors, such as CD151, which provide a clue

about the pathogenesis of pulmonary fibrosis and represent novel targets for development of therapies.

Author disclosures are available with the text of this article at www.atsjournals.org.

Acknowledgment: The authors thank Dr. Yasuyuki Yokosaki (Hiroshima University, Japan) for helpful discussions and critical reading of the manuscript, and Dr. Hideshi Kaneko (Teijin Pharmaceutical Company, Japan) for helpful comments on the electron microscopy studies.

References

1. Selman M, King TE, Pardo A. Idiopathic pulmonary fibrosis: prevailing and evolving hypotheses about its pathogenesis and implications for therapy. *Ann Intern Med* 2001;134:136–151.
2. Gross TJ, Hunninghake GW. Idiopathic pulmonary fibrosis. *N Engl J Med* 2001;345:517–525.
3. King TE Jr, Pardo A, Selman M. Idiopathic pulmonary fibrosis. *Lancet* 2011;378:1949–1961.
4. Crosby LM, Waters CM. Epithelial repair mechanisms in the lung. *Am J Physiol Lung Cell Mol Physiol* 2010;298:L715–L731.
5. Levy S, Shoham T. Protein-protein interactions in the tetraspanin web. *Physiology (Bethesda)* 2005;20:218–224.
6. Hemler ME. Tetraspanin proteins mediate cellular penetration, invasion, and fusion events and define a novel type of membrane microdomain. *Annu Rev Cell Dev Biol* 2003;19:397–422.
7. Hemler ME. Targeting of tetraspanin proteins–potential benefits and strategies. *Nat Rev Drug Discov* 2008;7:747–758.
8. Wang HX, Li Q, Sharma C, Knoblich K, Hemler ME. Tetraspanin protein contributions to cancer. *Biochem Soc Trans* 2011;39:547–552.
9. Suzuki M, Tachibana I, Takeda Y, He P, Minami S, Iwasaki T, Kida H, Goya S, Kijima T, Yoshida M, *et al.* Tetraspanin CD9 negatively regulates lipopolysaccharide-induced macrophage activation and lung inflammation. *J Immunol* 2009;182:6485–6493.
10. Takeda Y, He P, Tachibana I, Zhou B, Miyado K, Kaneko H, Suzuki M, Minami S, Iwasaki T, Goya S, *et al.* Double deficiency of tetraspanins CD9 and CD81 alters cell motility and protease production of macrophages and causes chronic obstructive pulmonary disease-like phenotype in mice. *J Biol Chem* 2008;283:26089–26097.
11. Shigeta M, Sanzen N, Ozawa M, Gu J, Hasegawa H, Sekiguchi K. CD151 regulates epithelial cell-cell adhesion through PKC- and Cdc42-dependent actin cytoskeletal reorganization. *J Cell Biol* 2003;163:165–176.
12. Moribe H, Yochem J, Yamada H, Tabuse Y, Fujimoto T, Mekada E. Tetraspanin protein (TSP-15) is required for epidermal integrity in Caenorhabditis elegans. *J Cell Sci* 2004;117:5209–5220.
13. Xia H, Diebold D, Nho R, Perlman D, Kleidon J, Kahm J, Avdulov S, Peterson M, Nerva J, Bitterman P, *et al.* Pathological integrin signaling enhances proliferation of primary lung fibroblasts from patients with idiopathic pulmonary fibrosis. *J Exp Med* 2008;205:1659–1672.
14. Kim KK, Wei Y, Szekeres C, Kugler MC, Wolters PJ, Hill ML, Frank JA, Brumwell AN, Wheeler SE, Kreidberg JA, *et al.* Epithelial cell alpha3beta1 integrin links beta-catenin and Smad signaling to promote myofibroblast formation and pulmonary fibrosis. *J Clin Invest* 2009;119:213–224.
15. Takeda Y, Kazarov AR, Butterfield CE, Hopkins BD, Benjamin LE, Kaipainen A, Hemler ME. Deletion of tetraspanin Cd151 results in decreased pathologic angiogenesis in vivo and in vitro. *Blood* 2007; 109:1524–1532.
16. Miyado K, Yamada G, Yamada S, Hasuwa H, Nakamura Y, Ryu F, Suzuki K, Kosai K, Inoue K, Ogura A, *et al.* Requirement of CD9 on the egg plasma membrane for fertilization. *Science* 2000;287:321–324.
17. Oku H, Shimizu T, Kawabata T, Nagira M, Hikita I, Ueyama A, Matsushima S, Torii M, Arimura A. Antifibrotic action of pirfenidone and prednisolone: different effects on pulmonary cytokines and growth factors in bleomycin-induced murine pulmonary fibrosis. *Eur J Pharmacol* 2008;590:400–408.
18. Rice WR, Conkright JJ, Na CL, Ikegami M, Shannon JM, Weaver TE. Maintenance of the mouse type II cell phenotype in vitro. *Am J Physiol Lung Cell Mol Physiol* 2002;283:L256–L264.
19. Saiga H, Nishimura J, Kuwata H, Okuyama M, Matsumoto S, Sato S, Matsumoto M, Akira S, Yoshikai Y, Honda K, *et al.* Lipocalin 2-dependent inhibition of mycobacterial growth in alveolar epithelium. *J Immunol* 2008;181:8521–8527.
20. Raghu G, Collard HR, Egan JJ, Martinez FJ, Behr J, Brown KK, Colby TV, Cordier JF, Flaherty KR, Lasky JA, *et al.* An official ATS/ERS/JRS/ALAT statement: idiopathic pulmonary fibrosis: evidence-based guidelines for diagnosis and management. *Am J Respir Crit Care Med* 2011;183:788–824.
21. Border WA, Noble NA. Transforming growth factor beta in tissue fibrosis. *N Engl J Med* 1994;331:1286–1292.
22. Fujiwara H, Hayashi Y, Sanzen N, Kobayashi R, Weber CN, Emoto T, Futaki S, Niwa H, Murray P, Edgar D, *et al.* Regulation of mesodermal differentiation of mouse embryonic stem cells by basement membranes. *J Biol Chem* 2007;282:29701–29711.
23. Shintani Y, Maeda M, Chaika N, Johnson KR, Wheelock MJ. Collagen I promotes epithelial-to-mesenchymal transition in lung cancer cells via transforming growth factor-beta signaling. *Am J Respir Cell Mol Biol* 2008;38:95–104.
24. Kisseleva T, Brenner DA. Fibrogenesis of parenchymal organs. *Proc Am Thorac Soc* 2008;5:338–342.
25. Moore BB, Hogaboam CM. Murine models of pulmonary fibrosis. *Am J Physiol Lung Cell Mol Physiol* 2008;294:L152–L160.
26. Sachs N, Kreft M, van den Bergh Weerman MA, Beynon AJ, Peters TA, Weening JJ, Sonnenberg A. Kidney failure in mice lacking the tetraspanin CD151. *J Cell Biol* 2006;175:33–39.
27. Baleato RM, Guthrie PL, Gubler MC, Ashman LK, Roselli S. Deletion of CD151 results in a strain-dependent glomerular disease due to severe alterations of the glomerular basement membrane. *Am J Pathol* 2008;173:927–937.
28. Sachs N, Claessen N, Aten J, Kreft M, Teske GJ, Koeman A, Zuurbier CJ, Janssen H, Sonnenberg A. Blood pressure influences end-stage renal disease of Cd151 knockout mice. *J Clin Invest* 2012;122:348–358.
29. Cowin AJ, Adams D, Geary SM, Wright MD, Jones JC, Ashman LK. Wound healing is defective in mice lacking tetraspanin CD151. *J Invest Dermatol* 2006;126:680–689.
30. Lau LM, Wee JL, Wright MD, Moseley GW, Hogarth PM, Ashman LK, Jackson DE. The tetraspanin superfamily member CD151 regulates outside-in integrin alphaIIbbeta3 signaling and platelet function. *Blood* 2004;104:2368–2375.
31. Taskar VS, Coultas DB. Is idiopathic pulmonary fibrosis an environmental disease? *Proc Am Thorac Soc* 2006;3:293–298.
32. du Bois RM. Strategies for treating idiopathic pulmonary fibrosis. *Nat Rev Drug Discov* 2010;9:129–140.
33. Chien CW, Lin SC, Lai YY, Lin BW, Lee JC, Tsai SJ. Regulation of CD151 by hypoxia controls cell adhesion and metastasis in colorectal cancer. *Clin Cancer Res* 2008;14:8043–8051.
34. Tzouvelekis A, Harokopos V, Paparountas T, Oikonomou N, Chatziioannou A, Vilaras G, Tsiambas E, Karameris A, Bouros D, Aidinis V. Comparative expression profiling in pulmonary fibrosis suggests a role of hypoxia-inducible factor-1alpha in disease pathogenesis. *Am J Respir Crit Care Med* 2007;176:1108–1119.
35. Fujishima S, Shiomi T, Yamashita S, Yogo Y, Nakano Y, Inoue T, Nakamura M, Tasaka S, Hasegawa N, Aikawa N, *et al.* Production and activation of matrix metalloproteinase 7 (matrilysin 1) in the lungs of patients with idiopathic pulmonary fibrosis. *Arch Pathol Lab Med* 2010;134:1136–1142.
36. Li M, Krishnaveni MS, Li C, Zhou B, Xing Y, Banfalvi A, Li A, Lombardi V, Akbari O, Borok Z, *et al.* Epithelium-specific deletion of TGF-beta receptor type II protects mice from bleomycin-induced pulmonary fibrosis. *J Clin Invest* 2011;121:277–287.
37. Degryse AL, Tanjore H, Xu XC, Polosukhin VV, Jones BR, Boomershine CS, Ortiz C, Sherrill TP, McMahon FB, Gleaves LA, *et al.* TGFbeta signaling in lung epithelium regulates bleomycin-induced alveolar injury and fibroblast recruitment. *Am J Physiol Lung Cell Mol Physiol* 2011;300:L887–L897.
38. Willis BC, Liebler JM, Luby-Phelps K, Nicholson AG, Crandall ED, du Bois RM, Borok Z. Induction of epithelial-mesenchymal transition in alveolar epithelial cells by transforming growth factor-beta1: potential role in idiopathic pulmonary fibrosis. *Am J Pathol* 2005;166:1321–1332.
39. Scotton CJ, Chambers RC. Molecular targets in pulmonary fibrosis: the myofibroblast in focus. *Chest* 2007;132:1311–1321.
40. Kim KK, Kugler MC, Wolters PJ, Robillard L, Galvez MG, Brumwell AN, Sheppard D, Chapman HA. Alveolar epithelial cell mesenchymal

transition develops in vivo during pulmonary fibrosis and is regulated by the extracellular matrix. *Proc Natl Acad Sci USA* 2006;103:13180–13185.

41. Johnson JL, Winterwood N, DeMali KA, Stipp CS. Tetraspanin CD151 regulates RhoA activation and the dynamic stability of carcinoma cell-cell contacts. *J Cell Sci* 2009;122:2263–2273.
42. Ke AW, Shi GM, Zhou J, Huang XY, Shi YH, Ding ZB, Wang XY, Devbhandari RP, Fan J. CD151 amplifies signaling by integrin α6β1 to PI3K and induces the epithelial-mesenchymal transition in HCC cells. *Gastroenterology* 2011;140:1629–1641.e15.
43. Lammerding J, Kazarov AR, Huang H, Lee RT, Hemler ME. Tetraspanin CD151 regulates alpha6beta1 integrin adhesion strengthening. *Proc Natl Acad Sci USA* 2003;100:7616–7621.
44. Sterk LM, Geuijen CA, Oomen LC, Calafat J, Janssen H, Sonnenberg A. The tetraspan molecule CD151, a novel constituent of hemidesmosomes, associates with the integrin alpha6beta4 and may regulate the spatial organization of hemidesmosomes. *J Cell Biol* 2000;149:969–982.
45. Nishiuchi R, Sanzen N, Nada S, Sumida Y, Wada Y, Okada M, Takagi J, Hasegawa H, Sekiguchi K. Potentiation of the ligand-binding activity of integrin alpha3beta1 via association with tetraspanin CD151. *Proc Natl Acad Sci USA* 2005;102:1939–1944.
46. Sadej R, Romanska H, Kavanagh D, Baldwin G, Takahashi T, Kalia N, Berditchevski F. Tetraspanin CD151 regulates transforming growth factor beta signaling: implication in tumor metastasis. *Cancer Res* 2010;70:6059–6070.
47. Thomas AQ, Lane K, Phillips J III, Prince M, Markin C, Speer M, Schwartz DA, Gaddipati R, Marney A, Johnson J, *et al.* Heterozygosity for a surfactant protein C gene mutation associated with usual interstitial pneumonitis and cellular nonspecific interstitial pneumonitis in one kindred. *Am J Respir Crit Care Med* 2002;165:1322–1328.
48. Karamatic Crew V, Burton N, Kagan A, Green CA, Levene C, Flinter F, Brady RL, Daniels G, Anstee DJ. CD151, the first member of the tetraspanin (TM4) superfamily detected on erythrocytes, is essential for the correct assembly of human basement membranes in kidney and skin. *Blood* 2004;104:2217–2223.
49. Drab M, Verkade P, Elger M, Kasper M, Lohn M, Lauterbach B, Menne J, Lindschau C, Mende F, Luft FC, *et al.* Loss of caveolae, vascular dysfunction, and pulmonary defects in caveolin-1 gene-disrupted mice. *Science* 2001;293:2449–2452.
50. Wang XM, Zhang Y, Kim HP, Zhou Z, Feghali-Bostwick CA, Liu F, Ifedigbo E, Xu X, Oury TD, Kaminski N, *et al.* Caveolin-1: a critical regulator of lung fibrosis in idiopathic pulmonary fibrosis. *J Exp Med* 2006;203:2895–2906.
51. Samuel CS, Zhao C, Bathgate RA, Bond CP, Burton MD, Parry LJ, Summers RJ, Tang ML, Amento EP, Tregear GW. Relaxin deficiency in mice is associated with an age-related progression of pulmonary fibrosis. *FASEB J* 2003;17:121–123.
52. Koval M, Billaud M, Straub AC, Johnstone SR, Zarbock A, Duling BR, Isakson BE. Spontaneous lung dysfunction and fibrosis in mice lacking connexin 40 and endothelial cell connexin 43. *Am J Pathol* 2011; 178:2536–2546.
53. Bouros D, Antoniou KM. Current and future therapeutic approaches in idiopathic pulmonary fibrosis. *Eur Respir J* 2005;26:693–702.

INTERNAL MEDICINE

□ CASE REPORT □

A Case of Combined Sarcoidosis and Usual Interstitial Pneumonia

Kazunobu Tachibana[1,2], Toru Arai[1,2], Tomoko Kagawa[2], Shojiro Minomo[2], Masanori Akira[3], Masanori Kitaichi[4] and Yoshikazu Inoue[1]

Abstract

Sarcoidosis is a systemic granulomatous disease of unknown etiology with characteristic pulmonary lesions, which are often distributed in the upper lung fields. We describe a unique case of sarcoidosis with lower lung field-dominant reticular shadows. Three years after the diagnosis of sarcoidosis based on histologic findings of the mediastinal lymph nodes and transbronchial lung biopsy specimens, the patient developed acute respiratory failure and died. The autopsy showed usual interstitial pneumonia (UIP), with honeycombing and superimposed diffuse alveolar damage of the lungs. The findings suggest that the patient had both sarcoidosis and UIP, and that the UIP later progressed to acute exacerbation.

Key words: sarcoidosis, usual interstitial pneumonia, acute exacerbation

(Intern Med 51: 1893-1897, 2012)
(DOI: 10.2169/internalmedicine.51.7394)

Introduction

Sarcoidosis is a systemic granulomatous disease of unknown etiology. Its radiologic characteristics include reticular opacities that are distributed predominantly in the upper lung fields (1). The radiologic finding of lower zone-dominant reticular shadowing is encountered only rarely in sarcoidosis (2, 3); however, this pattern is one of the characteristics of idiopathic pulmonary fibrosis/usual interstitial pneumonia (IPF/UIP) (4). Some patients with IPF are known to experience an acute exacerbation following a period of chronic disease progression (5-8). We recently encountered a patient with both pulmonary sarcoidosis and UIP, who developed an acute exacerbation of the latter condition, leading to his death from acute respiratory failure. The patient's clinical course could not be explained solely by sarcoidosis, but mimicked IPF. Thus, this case may assist in understanding the potential for sarcoidosis and UIP comorbidity, as well as the pathogenesis of reticular opacities distributed predominantly in the lower lung fields in patients with sarcoidosis.

Case Report

A 62-year-old man, an ex-smoker, was admitted to the Kinki-Chuo Chest Medical Center for the assessment of abnormal chest X-ray and computed tomography (CT) findings in 2007. He had worked as a truck driver for 14 years (from the age of 23 until the age of 37 years) and as a building demolition worker for the subsequent 25 years (from the age of 37 years to 62 years). He reported a four-month history of dry cough and worsening of dyspnea on effort. His only other relevant medical history was fatty liver, and hyperuricemia, which was treated with allopurinol. He had used a down quilt on the bed since age 32. Physical examination on admission revealed no palpable surface lymph nodes, no finger clubbing, and no skin rash; however, fine crackles were heard on chest auscultation. Peripheral blood findings on admission were as follows: WBC count, 5,900/μL; lactate dehydrogenase (LDH), 255 IU/L; and C-reactive protein (CRP) 0.09 mg/dL. The levels of Krebs von den Lungen-6

[1]Department of Diffuse Lung Diseases and Respiratory Failure, National Hospital Organization Kinki-Chuo Chest Medical Center, Japan, [2]Department of Respiratory Medicine, National Hospital Organization Kinki-Chuo Chest Medical Center, Japan, [3]Department of Radiology, National Hospital Organization Kinki-Chuo Chest Medical Center, Japan and [4]Department of Pathology, National Hospital Organization Kinki-Chuo Chest Medical Center, Japan
Received for publication January 24, 2012; Accepted for publication April 2, 2012
Correspondence to Dr. Yoshikazu Inoue, giichi@kch.hosp.go.jp

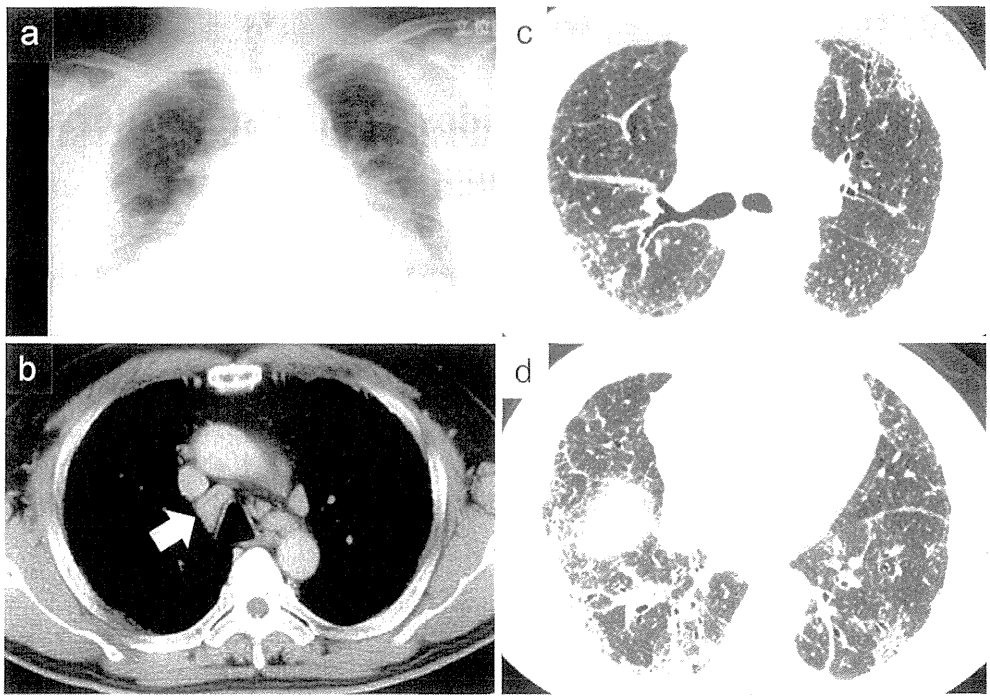

Figure 1. Chest radiograph (a) and CT scan (b-d) of the lung at the initial visit (2007), showing perilymphatic distributed small nodules, reticular opacities predominantly in the lower lung fields, and mediastinal lymphadenopathy (arrow).

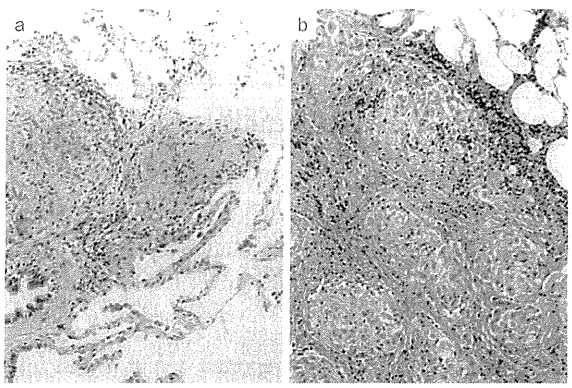

Figure 2. (a) The lung tissue of the right lower lobe (segment 8) was obtained by a transbronchoscopic biopsy in 2007. Epithelioid cell granulomas were formed in the wall of a respiratory bronchiole. Adjacent alveolar walls were relatively normal (Hematoxylin and Eosin staining, ×20). (b) The mediastinal lymph node was obtained by a mediastinoscopic biopsy in 2007. Numerous epithelioid cell granulomas were formed in the lymph node with perigranulomatous hyalinous fibrotic changes (Hematoxylin and Eosin staining, ×20). Based on the histologic evidence of the lung tissue and the mediastinal lymph node, the authors considered that the patient had sarcoidosis at the time of his initial visit in 2007.

(KL-6) and surfactant protein-D (SP-D) were increased (3,600 U/mL and 492 ng/mL, respectively), and an elevated activity of both angiotensin-converting enzyme (ACE) (25.1 U/lL; normal range: 8.3-21.4 U/L) and lysozyme (10.6 μg/mL; normal range: 5.0-10.2 μg/mL) was observed. The patient tested negative for antinuclear antibody and anti-double-stranded DNA. Tuberculin reaction was also negative.

Chest radiography revealed diffuse reticular opacities in the outer and lower zones of the lungs along with elevation of the diaphragm (Fig. 1a). A high-resolution CT scan of the chest demonstrated reticular shadows in the subpleural area, traction bronchiectasis, small nodules in perilymphatic and random distribution, and enlargement of the mediastinal lymph nodes (lower paratracheal lymph nodes) (Fig. 1b-d). Bronchoscopy revealed normal bronchial mucosa. Bronchoalveolar lavage (BAL) was performed in the right B^4b. The recovery rate of the bronchoalveolar lavage fluid (BALF) was 47%, and the total cell count in the fluid was 3.12×10^5/mL, with a breakdown of 45.8% macrophages, 16.3% lymphocytes, 11.7% neutrophils, and 26.2% eosinophils. The lymphocyte CD4/CD8 ratio was 7.41. No pathogen was detected in the BALF. Transbronchial biopsies of the right lung revealed noncaseating epithelioid cell granulomas in both S^3 and S^8 (Fig. 2a and data not shown). A mediastinoscopic biopsy of the mediastinal lymph nodes revealed numerous noncaseating epithelioid granulomas surrounded by hyalinous fibrotic changes (Fig. 2b). Based on these findings, a diagnosis of sarcoidosis involving the lungs and mediastinal lymph nodes was made. No sarcoidosis lesions were observed in other tissues including the heart, eyes and skin. At this time, the findings on chest X-ray and

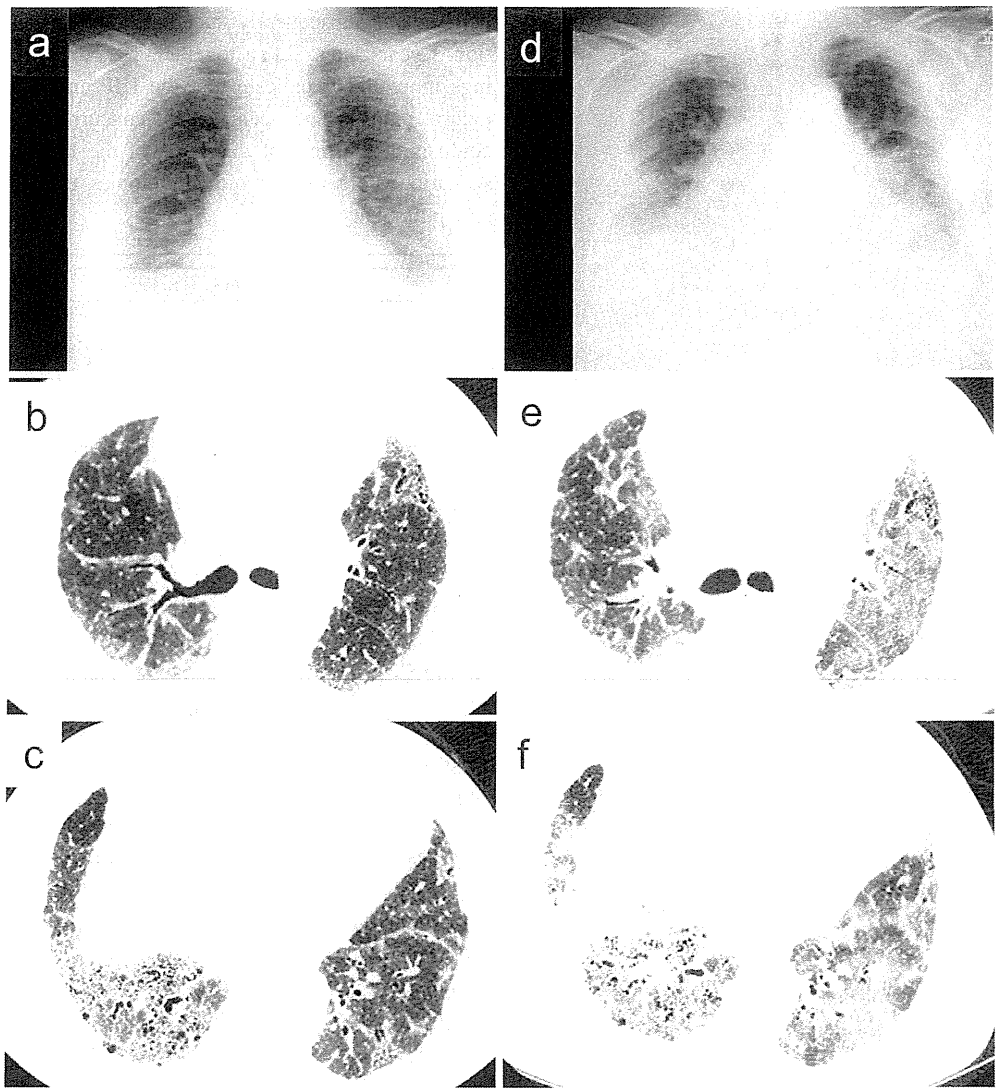

Figure 3. Chest radiograph (a) and CT scan (b, c) of the lung, 3 years after the initial visit (2007), showing progressed reticulation and volume loss. Chest radiograph (d) and CT scan (e, f) of the lung at the time of acute respiratory failure, showing diffuse ground glass opacities superimposed on reticular opacities.

on CT of the bilateral fibrotic lung lesions, predominantly in the lower lung zones, were considered to be due to the fibrotic lesions of sarcoidosis itself.

As treatment, 35 mg per day of oral prednisolone was started and then tapered. The patient's cough and dyspnea on exertion improved in two weeks, and an increase in vital capacity (VC) and diffusing capacity of the lung for carbon monoxide (DLco) were observed after a month, along with a slight improvement of small nodules in the lung detected on high-resolution CT and a decrease in the level of serum ACE. However, 20 months later, the patient experienced increasing shortness of breath, and chest imaging showed worsening of fibrotic shadows. Red-brown papules also appeared on the patient's lower legs, and these were diagnosed as cutaneous sarcoidosis by a dermatologist. These findings were presumed to indicate progression of the patient's sarcoidosis, and he was therefore treated with 35 mg per day of oral prednisolone, combined with 100 mg per day of azathioprine for the first seven months, switched to 100 mg of cyclosporine for the latter four months of this period, and 50 mg per week of etanercept for the final three months. However, this treatment was unsuccessful in preventing progression of the disease (Fig. 3a-c). Three years and two months after the initial diagnosis of sarcoidosis, a mass shadow in the right lung (S^6) was noted on chest CT. A CT-guided needle biopsy revealed adenocarcinoma with thyroid transcription factor-1 (TTF-1)-positivity, suggestive of primary lung cancer.

One and a half months later, just before staging of the lung cancer, the patient presented with sudden onset of dyspnea and hemosputum. Chest X-ray and CT showed diffuse ground glass opacities (Fig. 3d-f) in both lungs. The

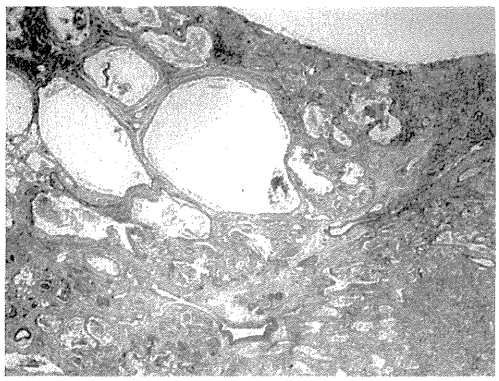

Figure 4. The lung tissue was obtained from the left lower lobe (segment 8) by an autopsy in 2010. The subpleural region (upper and left) showed cystic changes measuring 0.7-4 mm in diameter surrounded with fibrotic lesions (honeycombing). The inner lung parenchyma (lower and left) showed diffuse interstitial fibrotic thickening with temporal homogeneity. The authors considered the lung tissue as showing usual interstitial pneumonia (UIP) superimposed with fibrotic stage of diffuse alveolar damage (DAD). No granulomas were found (Hematoxylin and Eosin staining, ×1).

level of serum ACE remained normal. Treatment with high-dose corticosteroids, cyclophosphamide, antibiotics, and invasive positive-pressure ventilation was ineffective, and the patient died from respiratory failure 40 months after the initial diagnosis of sarcoidosis (nine days after the commencement of high-dose corticosteroid treatment).

An autopsy was performed, focusing on the thoracic and abdominal organs, which revealed multiple bilateral parietal pleural plaques (right: 50×50 mm, 20×20 mm; left: 45×20 mm, 40×12 mm, 30×15 mm, 40×12 mm). Eighty-three paraffin blocks were prepared for histopathologic diagnosis, including 14 from the right lung, 13 from the left lung, 4 from the mediastinal lymph nodes, and 2 each from the right and left parietal pleural plaque regions. We diagnosed the lung tissues as showing an UIP pattern, with honeycombing and superimposed diffuse alveolar damage (DAD) (Fig. 4). Asbestos bodies were not detected histologically, even after Prussian blue iron staining of the lung specimens. Therefore, bilateral lung tissues from the upper and lower lobes (right S^2, right S^{10}, left S^{1+2}, and left S^{10}) were measured for asbestos bodies. A total of 328 asbestos bodies per gram of dry weight of lung tissue were detected in the left lower lobe (S^{10}). The Helsinki Criteria for significant or occupational asbestos exposure is >1,000 asbestos bodies per gram of dry weight of lung tissue (9). Poorly differentiated adenocarcinoma (20×19×15 mm in size) was observed in the right lung (S^6), and metastatic carcinoma was noted in the right pleura, liver, and the pulmonary hilar and mediastinal lymph nodes. However, no granulomas were found in the examined tissues.

Based on these findings, we concluded that the patient suffered from sarcoidosis and UIP during the observation period, and subsequently succumbed to an acute exacerbation 3 years later. Taken together, we propose that our findings more likely indicate that the UIP and bilateral parietal pleural plaques had been present concurrently with the sarcoidosis at the time of diagnosis of the latter, rather than a scenario where the sarcoid granulomas underwent progressive pulmonary fibrosis.

Discussion

We have described a patient with evidence of both sarcoidosis and UIP characterized by lower lung field-predominant pulmonary fibrosis, who developed an acute exacerbation 3 years after the initial diagnosis of sarcoidosis.

The patient died from acute respiratory failure. It is possible that this was acute respiratory failure due to sarcoidosis (10-13), in which severe alveolitis with inflammatory or organized exudates in some alveolar spaces and noncaseating epithelioid granulomas are observed (14). However, this is unlikely in the present case for a number of reasons: (i) the autopsy revealed no granulomas in the lungs and lymph nodes, but rather showed diffuse alveolar damage superimposed on UIP; (ii) the level of serum ACE remained in the normal range; and, (iii) in cases of acute respiratory failure due to sarcoidosis, granulomas are usually observed in the lung despite having been treated with corticosteroids (14). As a result, we consider it more likely that this case was an acute exacerbation that developed during the course of UIP rather than acute respiratory failure due to sarcoidosis.

Radiographic and histologic findings suggest that the patient had both sarcoidosis and UIP. There are two possibilities: that the sarcoidosis and UIP existed concurrently; or that the fibrotic lesions developed as a fibrotic stage of sarcoidosis. For instance, Nobata et al. have reported a case of pulmonary sarcoidosis with UIP distributed predominantly in the lower lung fields. They noted the possibility of a fibrotic stage of pulmonary sarcoidosis (3) because the fibrosis was distributed along the bronchovascular bundles, which is a feature of the fibrotic stage of pulmonary sarcoidosis (15). In the present case, however, it is thought that the acute exacerbation developed during the chronic course of UIP as mentioned above. This theory is supported by the fact that the autopsy revealed no concentric fibrosis or concentric lamellar calcifications (Schumann bodies), which are characteristic of the fibrotic stage of sarcoidosis (16). Moreover, fibrotic lesions caused by sarcoidosis are predominantly distributed in the upper lung fields; 68% of sarcoidosis cases had fibrotic lesions predominantly in the upper lung fields, with no more than 4.5% of cases in the lower lung fields (2). As noted, in the present case, the UIP lesions were predominantly distributed in the lower lung fields. Taken together, these findings lead us to suggest that the present patient was concurrently suffering from both sarcoidosis and UIP.

During the course of observation, the patient had been

suspected of having chronic hypersensitivity pneumonia because of his history of using a down quilt on the bed. However, cessation of the use of down quilt neither improved the patient's condition nor stopped the disease progression. In addition, numerous well-developed granulomas were observed in the mediastinal lymph nodes (Fig. 2b). These findings therefore did not support the likelihood of chronic hypersensitivity pneumonia.

The autopsy showed parietal pleural plaques bilaterally, suggesting asbestos exposure. In general, asbestosis (a kind of lung fibrosis) is associated with a high level of exposure to asbestos (9). Unlike the present case, patients with asbestosis generally have a significant asbestos fiber burden and more extensive pleural plaques, which may be detected on chest CT (9). We believe that this patient probably had UIP and associated bilateral parietal pleural plaques as a result of his long duration of low-dose exposure to asbestos fibers, although progression of asbestosis is generally slow, the ten-year survival rate being around 70% (17, 18). This raises the possibility that the low-dose asbestos exposure might have caused sarcoid-like reaction as reported in cases of high-dose asbestos exposure (19, 20).

In summary, we have presented here a case of combined sarcoidosis and UIP with an acute exacerbation. This case is important in highlighting the possibility that sarcoidosis may develop after long-standing pulmonary fibrosis. Additional cases of lower lung field-predominant sarcoidosis should be studied in the future in order to further develop our understanding of this condition.

The authors state that they have no Conflict of Interest (COI).

Acknowledgement

The authors are grateful to Mr. Tomoaki Teramoto for performing the measurement of asbestos bodies from the lung tissues. This report was partially supported by a grant to the Diffuse Lung Diseases Research Group from the Ministry of Health, Labour and Welfare, Japan, and a grant from National Hospital Organization Respiratory Network.

References

1. Primack SL, Hartman TE, Hansell DM, Muller NL. End-stage lung disease: CT findings in 61 patients. Radiology **189**: 681-686, 1993.
2. Brauner MW, Grenier P, Mompoint D, Lenoir S, de Cremoux H. Pulmonary sarcoidosis: evaluation with high-resolution CT. Radiology **172**: 467-471, 1989.
3. Nobata K, Kasai T, Fujimura M, et al. Pulmonary sarcoidosis with usual interstitial pneumonia distributed predominantly in the lower lung fields. Intern Med **45**: 359-362, 2006.
4. Staples CA, Muller NL, Vedal S, Abboud R, Ostrow D, Miller RR. Usual interstitial pneumonia: correlation of CT with clinical, functional, and radiologic findings. Radiology **162**: 377-381, 1987.
5. Akira M, Hamada H, Sakatani M, Kobayashi C, Nishioka M, Yamamoto S. CT findings during phase of accelerated deterioration in patients with idiopathic pulmonary fibrosis. AJR Am J Roentgenol **168**: 79-83, 1997.
6. Collard HR, Moore BB, Flaherty KR, et al. Acute exacerbations of idiopathic pulmonary fibrosis. Am J Respir Crit Care Med **176**: 636-643, 2007.
7. Kondoh Y, Taniguchi H, Kawabata Y, Yokoi T, Suzuki K, Takagi K. Acute exacerbation in idiopathic pulmonary fibrosis. Analysis of clinical and pathologic findings in three cases. Chest **103**: 1808-1812, 1993.
8. Tachibana K, Inoue Y, Nishiyama A, et al. Polymyxin-B hemoperfusion for acute exacerbation of idiopathic pulmonary fibrosis: serum IL-7 as a prognostic marker. Sarcoidosis Vasc Diffuse Lung Dis **28**: 113-122, 2011.
9. Asbestos, asbestosis, and cancer: the Helsinki criteria for diagnosis and attribution. Scand J Work Environ Health **23**: 311-316, 1997.
10. Gupta D, Agarwal R, Paul AS, Joshi K. Acute hypoxemic respiratory failure in sarcoidosis: case report and review of the literature. Respir Care **56**: 1849-1852, 2011.
11. Leiba A, Apter S, Leiba M, Thaler M, Grossman E. Acute respiratory failure in a patient with sarcoidosis and immunodeficiency: an unusual presentation and a complicated course. Lung **182**: 73-77, 2004.
12. Pugazhenthi M. Sarcoidosis presenting as acute respiratory failure. South Med J **98**: 265, 2005.
13. Sabbagh F, Gibbs C, Efferen LS. Pulmonary sarcoidosis and the acute respiratory distress syndrome (ARDS). Thorax **57**: 655-656, 2002.
14. Shibata S, Saito K, Ishiwata N, Ieki R. A case of sarcoidosis presenting with high fever and rash progressing to acute respiratory failure. Nihon Kokyuki Gakkai Zasshi **45**: 691-697, 2007 (in Japanese, Abstract in English).
15. Padley SP, Padhani AR, Nicholson A, Hansell DM. Pulmonary sarcoidosis mimicking cryptogenic fibrosing alveolitis on CT. Clin Radiol **51**: 807-810, 1996.
16. Fraser RS, Muller NL, Colman N, Pare PD. Fraser and Pare's Diagnosis of Diseases of the Chest. 4th ed. W.B. Saunders, Philadelphia, 1999.
17. Coutts II, Gilson JC, Kerr IH, Parkes WR, Turner-Warwick M. Mortality in cases of asbestosis diagnosed by a pneumoconiosis medical panel. Thorax **42**: 111-116, 1987.
18. Markowitz SB, Morabia A, Lilis R, Miller A, Nicholson WJ, Levin S. Clinical predictors of mortality from asbestosis in the North American Insulator Cohort, 1981 to 1991. Am J Respir Crit Care Med **156**: 101-108, 1997.
19. Kido M, Kajiki A, Hiraoka K, Horie A. Sarcoid reaction observed in a worker with a history of asbestos exposure. J UOEH **12**: 355-360, 1990.
20. Granel B, Serratrice J, Disdier P, et al. Sarcoid-like pulmonary lesions during asbestosis. A case report. Sarcoidosis Vasc Diffuse Lung Dis **17**: 297, 2000.

Annals of Oncology 24: 54–59, 2013
doi:10.1093/annonc/mds214
Published online 11 September 2012

Updated overall survival results from a randomized phase III trial comparing gefitinib with carboplatin–paclitaxel for chemo-naïve non-small cell lung cancer with sensitive EGFR gene mutations (NEJ002)

A. Inoue[1*], K. Kobayashi[2], M. Maemondo[3], S. Sugawara[4], S. Oizumi[5], H. Isobe[6], A. Gemma[7], M. Harada[8], H. Yoshizawa[9], I. Kinoshita[10], Y. Fujita[11], S. Okinaga[12], H. Hirano[13], K. Yoshimori[14], T. Harada[15], Y. Saijo[16], K. Hagiwara[17], S. Morita[18] & T. Nukiwa[1] for the North-East Japan Study Group

[1]Department of Respiratory Medicine, Tohoku University Hospital, Sendai; [2]Department of Respiratory Medicine, Saitama Medical University International Medical Center, Saitama; [3]Department of Respiratory Medicine, Miyagi Cancer Center, Miyagi; [4]Department of Pulmonary Medicine, Sendai Kousei Hospital, Sendai; [5]First Department of Medicine, Hokkaido University School of Medicine, Sapporo; [6]Department of Medical Oncology, KKR Sapporo Medical Center, Sapporo; [7]Department of Internal Medicine, Division of Pulmonary Medicine, Infections Disease and Oncology, Nipppon Medical School, Tokyo; [8]Department of Respiratory Medicine, National Hospital Organization Hokkaido Cancer Center, Sapporo; [9]Bioscience Medical Research Center, Niigata University Medical & Dental Hospital, Niigata; [10]Department of Medical Oncology, Hokkaido University Graduate School of Medicine, Sapporo; [11]Department of Respiratory Medicine, National Hospital Organization Asahikawa Medical Center, Asahikawa; [12]Department of Respiratory Medicine, Kesennuma City Hospital, Miyagi; [13]Department of Respiratory Medicine, Iwate Prefectural Central Hospital, Morioka; [14]Division of Pulmonary Medicine, Anti-Tuberculosis Association Fukujuji Hospital, Tokyo; [15]Center for Respiratory Diseases, Hokkaido Social Insurance Hospital, Sapporo; [16]Department of Medical Oncology, Graduate School of Medicine, Hirosaki University, Hirosaki; [17]Department of Respiratory Medicine, Saitama Medical University, Saitama; [18]Department of Biostatistics and Epidemiology, Yokohama City University Medical Center, Yokohama, Japan

Received 7 March 2012; revised 26 May 2012; accepted 30 May 2012

Background: NEJ002 study, comparing gefitinib with carboplatin (CBDCA) and paclitaxel (PTX; Taxol) as the first-line treatment for advanced non-small cell lung cancer (NSCLC) harboring an epidermal growth factor receptor (EGFR) mutation, previously reported superiority of gefitinib over CBDCA/PTX on progression-free survival (PFS). Subsequent analysis was carried out mainly regarding overall survival (OS).

Materials and methods: For all 228 patients in NEJ002, survival data were updated in December, 2010. Detailed information regarding subsequent chemotherapy after the protocol treatment was also assessed retrospectively and the impact of some key drugs on OS was evaluated.

Results: The median survival time (MST) was 27.7 months for the gefitinib group, and was 26.6 months for the CBDCA/PTX group (HR, 0.887; $P = 0.483$). The OS of patients who received platinum throughout their treatment ($n = 186$) was not statistically different from that of patients who never received platinum ($n = 40$). The MST of patients treated with gefitinib, platinum, and pemetrexed (PEM) or docetaxel (DOC, Taxotere; $n = 76$) was around 3 years.

Conclusions: No significant difference in OS was observed between gefitinib and CBDCA/PTX in the NEJ002 study, probably due to a high crossover use of gefitinib in the CBDCA/PTX group. Considering the many benefits and the risk of missing an opportunity to use the most effective agent for EGFR-mutated NSCLC, the first-line gefitinib is strongly recommended.

Key words: EGFR mutation, gefitinib, individualized treatment, lung cancer

introduction

Two pivotal studies have revealed that somatic mutations in the kinase domain of the epidermal growth factor receptor (EGFR) strongly correlate with responsiveness to gefitinib, the first EGFR tyrosine kinase inhibitor (EGFR-TKI) used to treat non-small cell lung cancer (NSCLC) [1, 2]; subsequently, several phase II studies have demonstrated the promising efficacy of individualized treatment for advanced NSCLC patients with EGFR-TKI on the basis of EGFR gene mutation status [3–10]. Subsequently, we have conducted a phase III

Correspondence to: Dr A. Inoue, Department of Respiratory Medicine, Tohoku University Hospital, 1-1, Seiryomachi, Aobaku, Sendai, 980-8574, Japan. Tel: +81-22-717-8539; Fax: +81-22-717-8549; E-mail: akinoue@idac.tohoku.ac.jp

study comparing gefitinib with the standard platinum doublet regimen, carboplatin (CBDCA, Nippon Kayaku, Tokyo) and paclitaxel (PTX, Bristol-Myers Squibb, Tokyo), as the first-line treatment for advanced NSCLC harboring EGFR gene mutations (NEJ002) [11]. The study revealed that gefitinib provided significantly longer progression-free survival (PFS), the primary endpoint of the study, than CBDCA/PTX. Other phase III studies also have demonstrated the superiority of EGFR-TKI over the platinum doublet regimen [12, 13]; thus EGFR-TKIs are now globally recognized as the standard first-line treatment for advanced NSCLC with sensitive EGFR mutations [14].

Regarding overall survival (OS), one of the secondary endpoints of NEJ002, the rate of events was <40% in the previous report, for which the data cutoff point was December 2009. Although our study was not powered for OS, we proceeded with this OS analysis to evaluate the long-term survival result for each treatment group. We updated the data for PFS, OS, and safety examined in a longer follow-up period and also assessed the impact of subsequent chemotherapy on OS in patients with EGFR-mutated NSCLC.

materials and methods

study design and treatment

Full details of the NEJ002 study have been published previously. Eligible patients had chemo-naïve advanced NSCLC with a sensitive EGFR mutation detected by the highly sensitive peptide nucleic acid-locked nucleic acid PCR clamp method [15]. Patients were randomly assigned (1:1) to gefitinib (250 mg/day) or CBDCA (AUC 6.0)/paclitaxel (Taxol, 200 mg/m^2) on day 1 every 3 weeks (up to six cycles). The primary endpoint of NEJ002 was to evaluate the superiority of gefitinib over CBDCA/PTX in PFS. The secondary endpoints included response rate, OS, quality of life (QOL), and safety profiles (see Supplementary data, available at *Annals of Oncology* online). Patients provided a written informed consent. The study was conducted in accordance with the Helsinki Declaration of the World Medical Association. The protocol was approved by the institutional review board of each participating institution.

updated evaluation

PFS, OS, and safety data evaluated by the Common Terminology Criteria for Adverse Events version 3.0 were re-evaluated at the data cutoff point in December 2010 for the entire intent-to-treat population (n = 228), which was initially unplanned. Detailed information on subsequent chemotherapy carried out after the protocol treatment was also assessed for all patients retrospectively.

statistical analysis

The Kaplan–Meier survival curves were drawn for PFS and OS and compared using a two-sided non-stratified log-rank test with a significance level of 0.05. The hazard ratio (HR, gefitinib:CBDCA/PTX) and its two-sided 95% confidence interval (CI) were calculated by Cox regression analysis including only the treatment arm as a covariate. Subgroup analyses for OS, which were shown in a forest plot, were carried out to examine the interaction effect of treatment arm with age, gender, performance status, smoking status, type of histology, and type of EGFR mutation using a Cox regression model including treatment arm, each of the clinical factors, and their interaction effects as covariates. We did not account for adjustment for multiplicity due to the repetition of subgroup analyses, because we carried out them as exploratory analyses. Other comparative analyses were evaluated on the basis of a two-sided 5% significance level and 95% CI. All analyses were carried out using SAS for Windows release 9.1 (SAS Institute Inc., Cary, NC, USA).

Results

updated PFS

Among the 224 patients assessable, the updated median PFS of the gefitinib group and that of the CBDCA/PTX group were 10.8 months and 5.4 months, respectively (HR, 0.322; 95% CI 0.236–0.438; $P < 0.001$), which was quite similar to the previous results (Table 1). The number of events for PFS at the last data cutoff (December 2010) was 98 in the gefitinib group and 101 in the CBDCA/PTX group. The rate of events for PFS slightly increased from the previous report (from 83% to 88%).

updated OS

At the last data cutoff point, the median follow-up time was 704 days (range 30–1659) and 69 death events were observed in each arm. The rate of events for OS increased from 36% in the previous report to 61% in the current study (Table 1). The MST and the 2-year survival rate were 27.7 months and 58%,

Table 1. Previous and updated results of survival

	Previous results (in 2009)		Updated results (in 2010)	
First-line treatment group	Gefitinib	CBDCA/PTX	Gefitinib	CBDCA/PTX
PFS				
Median PFS, months	10.8	5.4	10.8	5.4
Hazard ratio (95% CI)	0.296 (0.215–0.408)		0.322 (0.236–0.438)	
One-year PFS rate	42.1%	3.2%	43.8%	4.2%
Number of events (%)	87 (76%)	100 (91%)	98 (86%)	101 (92%)
Overall survival				
Median survival time, months	30.5	23.6	27.7	26.6
Hazard ratio (95% CI)	0.798 (0.517–1.232)		0.887 (0.634–1.241)	
1-year survival rate	84.7%	86.4%	85.0%	86.8%
2-year survival rate	61.4%	46.7%	57.9%	53.7%
Number of events (%)	39 (34%)	43 (38%)	69 (61%)	69 (61%)

CBDCA/PTX, carboplatin plus paclitaxel; CI, confidence interval; PFS, progression-free survival.

respectively, for the gefitinib group, and 26.6 months and 54% for the CBDCA/PTX group (HR, 0.887; 95% CI 0.634–1.241; $P = 0.483$) (Figure 1). No factor, including the type of EGFR mutation, had a substantial impact on OS between the groups (Figure 2).

safety

No additional serious adverse event (NCI-CTC grade ≥3) was reported in either group after the previous report. Briefly, the most common adverse events reported were rash and diarrhea with gefitinib, and appetite loss, sensory neuropathy, and myelotoxicities with CBDCA/PTX. The combined incidence of serious adverse events combined was significantly higher in the CBDCA/PTX group than in the gefitinib group (71.7% versus 41.2%; $P < 0.001$).

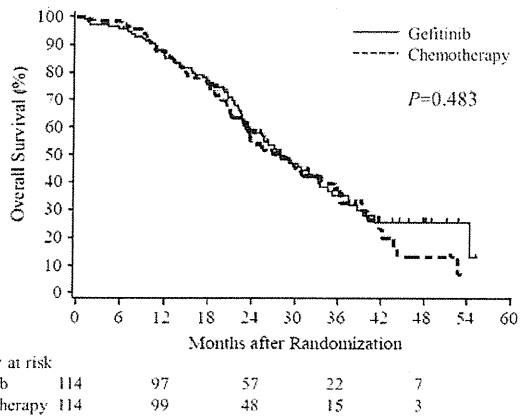

Figure 1. Kaplan–Meier curves for updated overall survival (OS) in the intent-to-treat population of NEJ002.

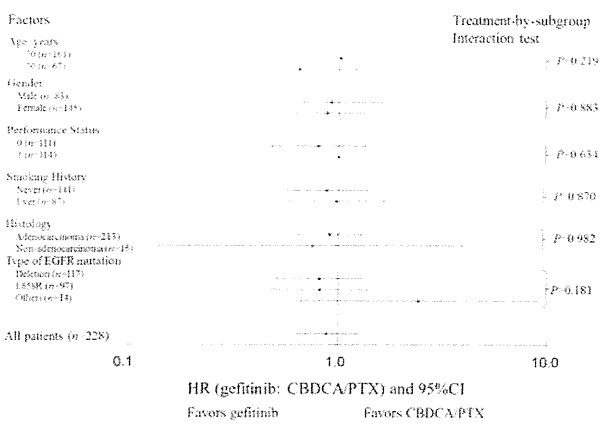

Figure 2. Forest plot of updated overall survival (OS) by clinical factors and the type of epidermal growth factor receptor (EGFR) mutation. Hazard ratio (HR) <1 implies a lower risk of death for patients treated with first-line gefitinb.

post-protocol chemotherapy

The chemotherapy regimens employed in NEJ002 are summarized in Table 2. Regarding the number of subsequent regimens, >50% of patients had received third-line chemotherapy or more, which was quite compatible with general practice in Japan (Figure 3A).

In the gefitinib group, 82 patients (72%) received at least one subsequent regimen. Among these, 74 patients (65%) were treated with the platinum doublet regimen including a crossover use of CBDCA/TXL in 59 patients (52%). Some patients received pemetrexed (PEM) combined with a platinum agent because it became available for the treatment of NSCLC in Japan in May 2009. Twelve patients went back on gefitinib and 32 received erlotinib in one of their later-line treatments. Among the 32 patients who received no subsequent regimen, 12 (11%) had been still treated with their first-line gefitinib at the data cutoff point (8 patients had still maintained their response to gefitinib, while 4 had continued gefitinib after the documentation of disease progression, in accordance with the patient's wishes). There were various reasons why the other 20 patients (18%) did not receive any subsequent regimens: deterioration of PS due to the progression of NSCLC ($n = 11$), interstitial lung disease due to gefitinib treatment ($n = 3$), exacerbation of co-morbidities ($n = 2$), or in accordance with the patient's wishes ($n = 4$). On the other hand, 113 patients (99%) in the CBDCA/PTX group had received at least one subsequent regimen, of whom 112 (98%) had moved to gefitinib.

The standard second-line chemotherapeutic agents PEM or docetaxel (DOC, Sanofi-Aventis K.K., Tokyo), which are used for advanced NSCLC, were used in 29% and 25% of patients in the gefitinib group, respectively, and in 16% and 19% of those in the CBDCA/PTX group, respectively. More than >20% of patients in both the arms received other agents such as irinotecan, S-1, gemcitabine, vinorelbine, or amrubicin as third- or later-line chemotherapy.

evaluation of the impact of key drugs on OS

To examine the impact of the platinum agent on OS of patients with EGFR-mutated NSCLC, we compared the OS of patients who received both gefitinib and a platinum agent in their treatment ($n = 186$) with that of patients who had never received a platinum agent ($n = 40$) in NEJ002. We found no significant difference between the OS of each group (Figure 3B). The number of patients who received a platinum agent but had not received gefitinib was only two in NEJ002.

We then assessed the impact of standard second-line agents (PEM and DOC) on OS. We divided patients who had received third-line or more in NEJ002 ($n = 131$) into two groups: the first group received EGFR-TKI, platinum agent, and PEM or DOC (P/D group, $n = 76$), and the second group received EGFR-TKI, platinum agent, but neither PEM nor DOC (no P/D group, $n = 55$). The MST of the P/D group was significantly longer than that of the no P/D group (34.8 months versus 22.6 months, $P = 0.003$) (Figure 3C).

Table 2. Summary of regimens for entire treatment in NEJ002

	Second-line *n* (%)	Third- or later-line *n* (%)	Total *n* (%)
First-line gefitinib group ($n = 114$)			
EGFR-TKI	8 (7.0)	34 (29.8)	114 (100)
Gefitinib	2 (1.8)	10 (8.8)	114 (100)
Erlotinib	6 (5.3)	26 (22.8)	32 (28.1)
Chemotherapy	74 (64.9)	52 (45.6)	76 (66.7)
Platinum based	71 (62.3)	11 (9.6)	74 (64.9)
CBDCA/PTX[a]	56 (49.2)	3 (2.6)	59 (51.8)
Platinum/PEM[b]	11 (9.6)	4 (3.5)	15 (13.2)
PEM (monotherapy)	2 (1.8)	16 (14.0)	18 (15.8)
DOC	0	28 (24.6)	28 (24.6)
Others[c]	1 (0.9)	26 (22.8)	27 (23.7)
First-line CBDCA/PTX group ($n = 114$)			
EGFR-TKI	109 (95.6)	42 (36.8)	112 (98.2)
Gefitinib	109 (95.6)	8 (7.0)	112 (98.2)
Erlotinib	0	33 (28.9)	33 (28.9)
BIBW2992	0	2 (1.8)	2 (1.8)
Chemotherapy	3 (2.7)	52 (45.6)	114 (100)
Platinum based	2 (1.8)	9 (7.9)	114 (100)
CBDCA/PTX	1 (0.9)	1 (0.9)	114 (100)
Platinum/PEM	0	4 (3.5)	4 (3.5)
PEM (monotherapy)	0	14 (12.3)	14 (12.3)
DOC	1 (0.9)	21 (18.4)	22 (19.3)
Others[c]	0	26 (22.8)	26 (22.8)

CBDCA/PTX, carboplatin plus paclitaxel; PEM, pemetrexed; EGFR-TKI, epidermal growth factor receptor tyrosine kinase inhibitor; DOC, docetaxel.
[a]Includes two CBDCA/PTX plus bevacizumab.
[b]Includes one CBDCA/PEM plus bevacizumab.
[c]Includes irinotecan, S-1, gemcitabine, vinorelbine, and amrubicine.

discussion

Although the NEJ002 study met its primary endpoint, in that gefitinib was superior to CBDCA/PTX in PFS, OS data were also important in evaluating the efficacy of the entire treatment including the regimens investigated. The current updated analysis demonstrated that the treatment course initiated with gefitinib achieved OS at least equivalent to a traditional treatment course initiated with a platinum doublet regimen for patients with advanced NSCLC harboring a sensitive EGFR mutation. Since the median follow-up time increased from 17 months in the previous report to 23 months in the current analysis, the OS results should become more accurate. We have already reported that the QOL was significantly better in the gefitinib group than in the CBDCA/PTX group in NEJ002 [16]. Moreover, gefitinib attained a high response rate, rapid improvement of symptoms, and exhibited low toxicity. Taking these factors together, we recommend the use of gefitinib as the first-line treatment.

There is a conservative opinion which states that the platinum doublet regimen should still be used as the first-line treatment for advanced NSCLC. This is because there has been no prospective study showing superiority of first-line EGFR-TKI over platinum doublet regimens for OS. Furthermore, some retrospective analyses have suggested that EGFR-TKI might be similarly effective in EGFR-mutated NSCLC regardless of the line at which it is used [17]. However, it is very important to recognize from our study that, though almost 100% of patients in the CBDCA/PTX group crossed over to gefitinib, the OS curve of the first-line gefitinib group was not inferior to that of the CBDCA/PTX group. While the risk associated with missing the administration of platinum agents after first-line gefitinib may be of concern, our *post-hoc* analysis suggested that the impact of the platinum agent on OS would not be larger than that of EGFR-TKI for patients with EGFR-mutated NSCLC. Figure 3B shows the MST of patients treated without platinum to be >2 years, which is a quite favorable result compared with previous historical data obtained when EGFR-TKI was not available. Thus, we feel that it is a concern if the chance to use gefitinib is missed when chemotherapy is carried out as the first-line treatment. The extremely high crossover rate in NEJ002 is hard to attain in general practice. In fact, only 51.5% of patients in the first-line CBDCA/PTX group received subsequent EGFR-TKI in the IPASS study [12]. Thus, we strongly recommend that the best drug should be used in the first instance.

Patients in the first-line gefitinib group tend to be treated with PEM or DOC monotherapy more intensively; this was because we supposed that some of these did not receive platinum doublet treatment for various reasons. However, we consider that the ideal treatment strategy for appropriate patients is to make use of available standard drugs. The most important finding in the *post-hoc* analysis shown in Figure 3C was that patients treated with EGFR-TKIs, platinum, and

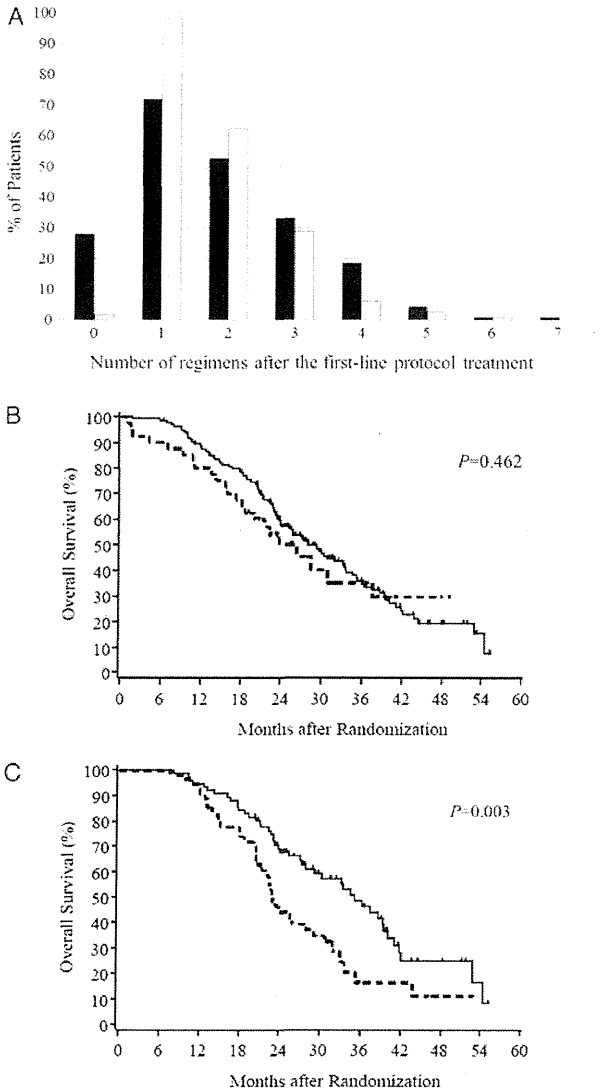

Figure 3. Evaluation of the impact of subsequent treatment on overall survival (OS) in NEJ002. The number of regimens that patients received after the first-line treatment with gefitinib (black bar) and that with chemotherapy (white bar) (A). The OS of patients treated with whichever line of gefitinib but not platinum (a dotted line) and those treated with both gefitinib and platinum (a solid line) (B). The OS of patients treated with gefitinib, platinum, with pemetrexed (PEM) and/or docetaxel (DOC; a solid line), and those treated with gefitinib, platinum but neither pemetrexed nor docetaxel (a dotted line) (C).

PEM/DOC achieved MST of around 3 years even though they had systemically advanced disease; however, the analysis may not conclusively show the difference between the two groups because they were not randomly assigned. This suggests that patients with EGFR-mutated NSCLC and with good PS enough to complete many lines of treatment may further benefit from a proper use of the above mentioned 'key drugs'. Although PEM and DOC were equally recognized as standard second-line agents at the time of the NEJ002 study [18], we now consider PEM to be more appropriate for EGFR-mutated NSCLC where adenocarcinoma is much common [14]. Since at least 14 patients (12%) failed to move to subsequent chemotherapy and ~20% of patients had never received platinum agents or PEM after their disease progressed in the gefitinib group, we think there may be a room for improvement of OS in these populations. Thus, we are now investigating a new treatment strategy, in which the first-line gefitinib is combined with CBDCA and PEM, for patients with EGFR-mutated NSCLC (UMIN000002789).

There are some limitations in the current analysis. First, the sample size of NEJ002 had inadequate power for evaluation of the difference in OS between the two groups. Since death events in one-third of patients have not yet occurred, the true OS curve may change slightly from that shown in this report. A meta-analysis combining several phase III studies and comparing EGFR-TKI with platinum doublet in an EGFR-mutated NSCLC population would be warranted. Second, the *post-hoc* analysis on subsequent chemotherapies may have been biased, because post-protocol treatments were not restricted under the NEJ002 protocol; however, they were very similar to those used in general practice in Japan. In addition, the unplanned comparative analysis between the subgroups shown in Figure 3B and C cannot draw definitive conclusions. It may be difficult to find whether the additive effect of platinum agents or PEM/DOC or good PS itself, that enabled patients to receive those agents irrespective of chemotherapy effects, influenced survival prolongation in the superior group more directly. However, we believe that they give us some interesting suggestions for future investigations such as that underway in our new study.

The reason there was no significant difference in OS between the first-line gefitinib group and the first-line CBDCA/PTX group in NEJ002 was very likely a high rate of crossover use of gefitinib in the CBDCA/PTX group. Considering the many benefits from EGFR-TKI use and the risk of missing an opportunity to use the most effective agent for treatment of EGFR-mutated NSCLC, the first-line gefitinib is strongly recommended in general practice for this population.

funding

This work is supported by grant-in-aids from Japan Society for Promotion of Science and Japanese Foundation for the Multidisciplinary Treatment of Cancer. This study is also supported by the Tokyo Cooperative Oncology Group.

disclosure

KK, AG, YS, and TN had received research grants from AstraZeneca. AI, KK, MM, HI, KH, and TN had received lecture fees from AstraZeneca. All remaining authors have declared no conflicts of interest.

references

1. Lynch TJ, Bell DW, Sordella R et al. Activating mutations in the epidermal growth factor receptor underlying responsiveness of non-small-cell lung cancer to gefitinib. N Engl J Med 2004; 350: 2129–2139.

2. Paez JG, Janne PA, Lee JC et al. EGFR mutations in lung cancer: correlation with clinical response to gefitinib therapy. Science 2004; 304: 1497–1500.
3. Inoue A, Suzuki T, Fukuhara T et al. Prospective phase II study of gefitinib for chemotherapy-naive patients with advanced non-small-cell lung cancer with epidermal growth factor receptor gene mutations. J Clin Oncol 2006; 24: 3340–3346.
4. Asahina H, Yamazaki K, Kinoshita I et al. A phase II trial of gefitinib as first-line therapy for advanced non-small cell lung cancer with epidermal growth factor receptor mutations. Br J Cancer 2006; 95: 998–1004.
5. Sutani A, Nagai Y, Udagawa K et al. Gefitinib for non-small-cell lung cancer patients with epidermal growth factor receptor gene mutations screened by peptide nucleic acid-locked nucleic acid PCR clamp. Br J Cancer 2006; 95: 1483–1489.
6. Tamura K, Okamoto I, Kashii T et al. Multicentre prospective phase II trial of gefitinib for advanced non-small cell lung cancer with epidermal growth factor receptor mutations: results of the west Japan thoracic oncology group trial (WJTOG0403). Br J Cancer 2008; 98: 907–914.
7. Sunaga N, Tomizawa Y, Yanagitani N et al. Phase II prospective study of the efficacy of gefitinib for the treatment of stage III/IV non-small cell lung cancer with EGFR mutations, irrespective of previous chemotherapy. Lung Cancer. 2007; 56: 383–389.
8. Yoshida K, Yatabe Y, Park JY et al. Prospective validation for prediction of gefitinib sensitivity by epidermal growth factor receptor gene mutation in patients with non-small cell lung cancer. J Thorac Oncol. 2007; 2: 22–28.
9. Sugio K, Uramoto H, Onitsuka T et al. Prospective phase II study of gefitinib in non-small cell lung cancer with epidermal growth factor receptor gene mutations. Lung Cancer 2009; 64: 314–318.
10. Morita S, Okamoto I, Kobayashi K et al. Combined survival analysis of prospective clinical trials of gefitinib for non-small cell lung cancer with EGFR mutations. Clin Cancer Res. 2009; 15: 4493–4498.
11. Maemondo M, Inoue A, Kobayashi K et al. Gefitinib or chemotherapy for non-small-cell lung cancer with mutated EGFR. N Engl J Med. 2010; 362: 2380–2388.
12. Mok T, Wu YL, Thongprasert S et al. Gefitinib or carboplatin–paclitaxel in pulmonary adenocarcinoma. N Engl J Med 2009; 361: 947–957.
13. Mitsudomi T, Morita S, Yatabe Y et al. Gefitinib versus cisplatin plus docetaxel in patients with non-small-cell lung cancer harbouring mutations of the epidermal growth factor receptor (WJTOG3405): an open label, randomised phase 3 trial. Lancet Oncol 2010; 11: 121–128.
14. Azzoli CG, Baker S, Temin S et al. American society of clinical oncology clinical practice guideline update on chemotherapy for stage IV non-small-cell lung cancer. J Clin Oncol 2009; 27: 6251–6266.
15. Nagai Y, Miyazawa H, Huqun M et al. Genetic heterogeneity of the epidermal growth factor receptor in non-small cell lung cancer cell lines revealed by a rapid and sensitive detection system, the peptide nucleic acid-locked nucleic acid PCR clamp. Cancer Res 2005; 65: 7276–7282.
16. Oizumi S, Kobayashi K, Inoue A et al. Quality of life with gefitinib in patients with EGFR-mutated non-small cell lung cancer: quality of life analysis of north east Japan study group 002 Trial. Oncologist 2012; 17: 863–870.
17. Rosell R, Moran T, Queralt C et al. Screening for epidermal growth factor receptor mutations in lung cancer. N Engl J Med 2009; 361: 958–967.
18. Hanna N, Shepherd FA, Fossella FV. Randomized phase III trial of pemetrexed versus docetaxel in patients with non-small-cell lung cancer previously treated with chemotherapy. J Clin Oncol 2004; 22: 1589–1597.

Annals of Oncology 24: 59–66, 2013
doi:10.1093/annonc/mds242
Published online 10 August 2012

Pemetrexed-based chemotherapy in patients with advanced, ALK-positive non-small cell lung cancer

A. T. Shaw[1]*, A. M. Varghese[2], B. J. Solomon[3], D. B. Costa[4], S. Novello[5], M. Mino-Kenudson[6], M. M. Awad[1], J. A. Engelman[1], G. J. Riely[2], V. Monica[5], B. Y. Yeap[1] & G. V. Scagliotti[5]

[1]Department of Medicine Hematology/Oncology, Massachusetts General Hospital Cancer Center, Boston; [2]Department of Thoracic Oncology, Memorial Sloan-Kettering Cancer Center, New York, USA; [3]Department of Medical Oncology, Peter MacCallum Cancer Centre, East Melbourne, Australia; [4]Division of Hematology/Oncology, Beth Israel Deaconess Medical Center, Boston, USA; [5]Department of Clinical and Biological Sciences, University of Torino, Torino, Italy; [6]Department of Pathology, Massachusetts General Hospital, Boston, USA

Received 16 May 2012; revised 11 June 2012; accepted 13 June 2012

Background: Anaplastic lymphoma kinase (ALK)-positive non-small-cell lung cancer (NSCLC) is highly responsive to crizotinib. To determine whether ALK-positive NSCLC is also sensitive to pemetrexed, we retrospectively evaluated progression-free survival (PFS) of ALK-positive versus ALK-negative patients who had been treated with pemetrexed-based chemotherapy for advanced NSCLC.

Patients and methods: We identified 121 patients with advanced, ALK-positive NSCLC in the USA, Australia, and Italy. For comparison, we evaluated 266 patients with advanced, ALK-negative, epidermal growth factor receptor (EGFR)-wild-type NSCLC, including 79 with KRAS mutations and 187 with wild-type KRAS (WT/WT/WT). We determined PFS on different pemetrexed regimens.

*Correspondence to: Dr A. T. Shaw, Thoracic Oncology, Massachusetts General Hospital Cancer Center, Yawkey 7B-7508, 32 Fruit Street, Boston, MA 02114, USA.
Tel: +1-617-724-4000; Fax: +1-617-726-0453; E-mail: ashaw1@partners.org

Published OnlineFirst August 20, 2012; DOI: 10.1158/1078-0432.CCR-11-2947

Clinical Cancer Research

Imaging, Diagnosis, Prognosis

A Prospective PCR-Based Screening for the *EML4-ALK* Oncogene in Non–Small Cell Lung Cancer

Manabu Soda[1], Kazutoshi Isobe[2], Akira Inoue[6], Makoto Maemondo[7], Satoshi Oizumi[8], Yuka Fujita[9], Akihiko Gemma[3], Yoshihiro Yamashita[1], Toshihide Ueno[1], Kengo Takeuchi[4], Young Lim Choi[1,5], Hitoshi Miyazawa[10], Tomoaki Tanaka[10], Koichi Hagiwara[10], and Hiroyuki Mano[1,5,11], for the North-East Japan Study Group and the ALK Lung Cancer Study Group

Abstract

Purpose: *EML4-ALK* is a lung cancer oncogene, and ALK inhibitors show marked therapeutic efficacy for tumors harboring this fusion gene. It remains unsettled, however, how the fusion gene should be detected in specimens other than formalin-fixed, paraffin-embedded tissue. We here tested whether reverse transcription PCR (RT-PCR)-based detection of *EML4-ALK* is a sensitive and reliable approach.

Experimental Design: We developed a multiplex RT-PCR system to capture *ALK* fusion transcripts and applied this technique to our prospective, nationwide cohort of non–small cell lung cancer (NSCLC) in Japan.

Results: During February to December 2009, we collected 916 specimens from 853 patients, quality filtering of which yielded 808 specimens of primary NSCLC from 754 individuals. Screening for *EML4-ALK* and *KIF5B-ALK* with our RT-PCR system identified *EML4-ALK* transcripts in 36 samples (4.46%) from 32 individuals (4.24%). The RT-PCR products were detected in specimens including bronchial washing fluid ($n = 11$), tumor biopsy ($n = 8$), resected tumor ($n = 7$), pleural effusion ($n = 5$), sputum ($n = 4$), and metastatic lymph node ($n = 1$). The results of RT-PCR were concordant with those of sensitive immunohistochemistry with ALK antibodies.

Conclusions: Multiplex RT-PCR was confirmed to be a reliable technique for detection of *ALK* fusion transcripts. We propose that diagnostic tools for *EML4-ALK* should be selected in a manner dependent on the available specimen types. FISH and sensitive immunohistochemistry should be applied to formalin-fixed, paraffin-embedded tissue, but multiplex RT-PCR is appropriate for other specimen types. *Clin Cancer Res; 18(20); 5682–9. ©2012 AACR.*

Introduction

An oncogenic fusion between the echinoderm microtubule-associated protein–like 4 gene (*EML4*) and the anaplastic lymphoma kinase gene (*ALK*) was discovered by functional screening with a non–small cell lung cancer (NSCLC) specimen (1). *EML4* and *ALK* are located within a short distance (~12 Mbp) of each other on the short arm of human chromosome 2, and a small inversion involving the 2 loci is responsible for generation of the *EML4-ALK* fusion in lung cancer. The EML4-ALK tyrosine kinase undergoes constitutive dimerization through a coiled-coil domain within EML4, resulting in kinase activation and conferring potent transforming ability (2, 3). Transgenic mice expressing *EML4-ALK* in lung alveolar cells develop multiple adenocarcinoma nodules soon after birth, but treatment with an ALK inhibitor results in the rapid clearance of such nodules, confirming the addiction of EML4-ALK–positive tumors to the kinase activity of the fusion protein (4). The therapeutic efficacy of ALK inhibitors has been confirmed in other transgenic mice expressing EML4-ALK (5).

Several ALK inhibitors have already entered clinical trials or are under preclinical development (6–10). Marked therapeutic efficacy of one such compound, crizotinib, has been described in patients with NSCLCs positive for *EML4-ALK*, with an overall response rate of 57% (7), and crizotinib was recently approved as a therapeutic drug by the U.S. Food

Authors' Affiliations: [1]Division of Functional Genomics, Jichi Medical University, Tochigi; [2]Department of Respiratory Medicine, Toho University Omori Medical Center; [3]Nippon Medical School Hospital; [4]Pathology Project for Molecular Targets, The Cancer Institute; [5]Department of Medical Genomics, Graduate School of Medicine, University of Tokyo, Tokyo; [6]Tohoku University Hospital; [7]Miyagi Cancer Center, Miyagi; [8]First Department of Medicine, Hokkaido University School of Medicine; [9]Asahikawa Medical Center, Hokkaido; [10]Saitama Medical University Hospital; and [11]CREST, Japan Science and Technology Agency, Saitama, Japan

Note: Supplementary data for this article are available at Clinical Cancer Research Online (http://clincancerres.aacrjournals.org/).

The nucleotide sequence of the novel *EML4-ALK* variant cDNA from patient J-#189 has been deposited in the DDBJ/EMBL/GenBank databases under the accession number AB663645.

Corresponding Author: Hiroyuki Mano, Division of Functional Genomics, Jichi Medical University, 3311-1 Yakushiji, Shimotsukeshi, Tochigi 329-0498, Japan. Phone: 81-285-58-7449; Fax: 81-285-44-7322; E-mail: hmano@jichi.ac.jp

doi: 10.1158/1078-0432.CCR-11-2947

Published OnlineFirst August 20, 2012; DOI: 10.1158/1078-0432.CCR-11-2947

Translational Relevance

The recent approval of an ALK inhibitor by the U.S. Food and Drug Administration has rendered urgent the development of a diagnostic scheme for tumors harboring *ALK* fusion genes. Whereas FISH is effective for analysis of formalin-fixed, paraffin-embedded (FFPE) tissue, how to test other types of specimen remains unsettled. We conducted a prospective, nationwide screening for *EML4-ALK*- or *KIF5B-ALK*–positive lung carcinomas in Japan with the use of a newly developed multiplex reverse transcription (RT)-PCR system. Various subtypes of *EML4-ALK* cDNA were identified in 36 of 808 specimens with adequate RNA quality. The RT-PCR results were concordant with those of immunohistochemistry, and *EML4-ALK* PCR products were detected in independent specimens from the same individuals. As far as we are aware, our study represents the first prospective RT-PCR–based screening for *EML4-ALK*, and it shows that multiplex RT-PCR is reliable for detection of the fusion gene in non-FFPE specimens.

and Drug Administration within a remarkably short period after target discovery (3, 11).

The failure of crizotinib treatment in individuals without oncogenic *ALK* fusions (12) and an adverse effect of treatment with gefitinib on the prognosis of patients with NSCLCs who do not harbor mutations of the EGF receptor (*EGFR*) gene (13) both suggest that ALK inhibitors should be administered only to patients positive for oncogenic ALK proteins. FISH-based detection of *ALK* rearrangements has proved to be of diagnostic use in the trials with crizotinib (7). Furthermore, detection of ALK proteins by sensitive immunohistochemistry (IHC) has been described (14, 15), and one such immunohistochemical screening approach resulted in the identification of another oncogenic ALK fusion, KIF5B-ALK (14). However, a substantial proportion of patients attending clinics are diagnosed with lung cancer on the basis of pathologic analysis of bronchial lavage fluid, pleural effusion, or sputum. Given that these specimens are not always suitable for the preparation of formalin-fixed, paraffin-embedded (FFPE) tissue required for FISH or IHC, individuals who are diagnosed solely by analysis of such specimens cannot receive EML4-ALK tests. To allow the sensitive detection of *EML4-ALK* and *KIF5B-ALK* in such specimens, we have now developed a multiplex reverse transcription (RT)-PCR system that captures the 2 *ALK* fusions, and we have tested its reliability as a diagnostic tool in our large-scale prospective cohort.

Materials and Methods

Prospective collection of NSCLC specimens

During February to December of 2009, we collected a total of 916 lung cancer specimens from 853 independent patients through our multicenter, nationwide networks in Japan. All specimens but resected tumors were mixed with RLT buffer (Qiagen) immediately after sampling, a step that markedly inhibits RNA degradation for up to 3 days at room temperature (data not shown). Resected tumor samples were snap-frozen and stored at −80°C until extraction of RNA and DNA. Portions of the samples were sent to Jichi Medical University (Tochigi, Japan) for multiplex RT-PCR analysis of *EML4-ALK* and *KIF5B-ALK* fusions and to Saitama Medical University (Saitama, Japan) for peptide nucleic acid–locked nucleic acid (PNA-LNA) PCR clamp analysis of *EGFR* mutations (16). All specimens were confirmed by pathologic analysis to contain malignant cells. More than half of the specimens were collected through the North-East Japan Study Group network according to the NEJ004 protocol. The study was approved by the Institutional Review Board of each participating center, and written informed consent was obtained from each study subject. All statistical analysis was conducted with 2-sided tests, and a $P < 0.05$ was considered statistically significant.

Clinicopathologic features of EML4-ALK–positive NSCLC

The clinicopathologic features of patients with *EML4-ALK*–positive or -negative tumors in our cohort are summarized in Table 1 and Supplementary Table S1. Consistent with previous observations, *EML4-ALK*–positive patients were significantly younger than those without *EML4-ALK* ($P < 0.001$, Student' t test) and were enriched in never or light smokers ($P < 0.001$, Fisher exact test). Our data also indicated that *EML4-ALK*–positive tumors are more likely to occur in women than in men ($P < 0.001$, Fisher exact test). In the present cohort, *EML4-ALK* was detected only in lung adenocarcinoma ($P < 0.001$, Fisher exact test), for which the fusion-positive rate was 6.11%.

A total of 718 specimens were screened for *EGFR* mutations, with such mutations being detected in 171 cases (23.8%). Whereas most *EML4-ALK*–positive tumors did not harbor *EGFR* mutations ($P = 0.002$, Fisher exact test), we did detect one tumor doubly positive in this regard. *EML4-ALK* and *EGFR* mutations are largely mutually exclusive (17, 18), but, importantly, such exclusiveness may not be absolute (19). Given that the presence of *EML4-ALK* and *EGFR* mutations in our doubly positive patient was examined with cells isolated from bronchial washing fluid, which was the only available specimen for molecular analysis in this individual, we were not able to determine whether there was a genuinely double-positive tumor in the lung or there were multiple independent tumors each positive for *EML4-ALK* or mutated *EGFR*.

We also attempted to examine the mutation status of *KRAS* among our 32 cases positive for *EML4-ALK*. We were able to sequence *KRAS* cDNAs for 26 of these patients, none of whom showed *KRAS* alterations (data not shown), confirming the mutual exclusivity of *EML4-ALK* and *KRAS* mutations (17, 20, 21).

Quality assessment of samples

Complementary DNA prepared from the specimens was first subjected to RT-PCR analysis with primers (5′-